Strål säkerhets myndigheten
Swedish Radiation Safety Authority

Author: Richard Kłos

Research

2015:47

GEMA-Site 1: Model description and example application

Report number: 2015:47 ISSN: 2000-0456
Available at www.stralsakerhetsmyndigheten.se

SSM perspective

Background

In 2011 the Swedish Nuclear Fuel and Waste Management Company (SKB) submitted an assessment of the long-term safety of a KBS-3 geological disposal facility for spent nuclear fuel in Forsmark, Sweden. This assessment, the SR-Site project, supports the licence application of SKB to build such a final disposal facility. The biosphere dose assessment carried out as part of SR-Site features a highly detailed model of the evolution of the landscape in Forsmark area. The Forsmark site is located on the Baltic coast with a terrestrial landscape including lakes, mires, forest and arable land. The land at the site is projected to continue to rise due to post-glacial uplift (legacy climate change from the previous deglaciation) leading to significant ecosystem transitions over the next ten to twenty thousand years. SKB's biosphere model is built on a landscape evolution model, whereby radionuclide releases to distinct hydrological basins/sub-catchments (termed "objects") are represented as they evolve through land rise.

Objective

The objective of the study is to develop an alternative evolving dose assessment model that is simple but includes relevant details of local characteristics, particularly in respect of changes to the near-surface hydrology during land rise. The developed model, GEMA-Site, is used by SSM to investigate uncertainties associated with the modelling of the future Forsmark landscape in the context of long timescale radiological assessment.

Results

GEMA-Site is configured to represent radionuclide transport and accumulation in the Swedish landscape (both present and future) around the planned location of a final repository for spent nuclear fuel at Forsmark. Doses potentially arising to local population groups are evaluated. The site-specific characteristics that influence the model definition are

- a rapidly evolving landscape as a result of landrise, a legacy of the previous glaciation,
- characterisation of a whole basin in the landscape with evolving ground water flow vectors in the near-surface regolith material,
- ecosystem transitions as the Baltic coast retreats, featuring marine, lacus trine, natural ecosystems (forest and wetland) as well as agricultural land,
- representation of the altered hydrology of the basin imposed by human action to facilitate agriculture, including the exploitation of water resources in the surface environment (lakes, surface drainage system and shallow wells).

Need for further research

The GEMA-site model can be further developed/improved in the following aspects:

- a better means of integrating results from hydrologic modelling to describe interactions between geosphere and biosphere,
- exposure pathways through use of local water resources,
- exposure pathways via the game consumption.

Project information

Contact person SSM: Shulan Xu
Reference: SSM 2014-1147

Strål
säkerhets
myndigheten
Swedish Radiation Safety Authority

Author: Richard Kłos
Aleksandria Sciences Ltd. Sheffield, UK.

2015:47

GEMA-Site 1: Model description and example application

Date: December 2015
Report number: 2015:47 **ISSN:** 2000-0456
Available at www.stralsakerhetsmyndigheten.se

This report concerns a study which has been conducted for the Swedish Radiation Safety Authority, SSM. The conclusions and viewpoints presented in the report are those of the author/authors and do not necessarily coincide with those of the SSM.

Contents

1. Introduction

In 2011 the Swedish Nuclear Fuel and Waste Management Company (SKB) submitted an assessment of the long-term safety of a KBS-3 geological disposal facility (GDF) for the disposal of spent nuclear fuel and high level radioactive waste in Forsmark, Sweden. This assessment, the SR-Site project, supports the licence application of SKB to build such a final disposal facility.

The biosphere dose assessment carried out as part of SR-Site features a highly detailed model of the evolution of the current sea area to the northeast of the planned repository location – the Öregrundsgrepen. Currently submerged, the landscape will emerge over the next few millennia as the land to the southwest has emerged since the end of the previous glaciation. The developing landscape can be assumed to evolve in much the same way. In this way the important transport and accumulation characteristics of the landscape and the patterns of human behaviour leading to potential future exposure to any radionuclides released from the disposal facility into the surface hydrological system can be modelled, employing a detailed site characterisation programme such as that carried out by SKB over the past decade.

The model employed in SKB's dose assessment calculations is described by Avila *et al*. (2010). This has been reviewed by Kłos *et al*. (2012) and in greater detail focussing *inter alia* on the interpretation of hydrology in the model and on the development of an alternative conceptual model for radionuclide transport and accumulation (Kłos *et al*., 2014). This report provides details of the development and initial application of the alternative model, known as GEMA-Site, reflecting SSM's complementary modelling project over the last decade (see Kłos, 2008). GEMA-Site and the use of simple Reference Biosphere-type models (Walke, 2014) have been used by SSM to investigate uncertainties associated with the modelling of the future Forsmark landscape in the context of long timescale radiological assessment.

The model described here gives the basic specification for the GEMA-Site conceptual model, using a simple approximation to the near-surface hydrology in a single basin in the landscape. The characterisation of the basin employs data taken from Avila *et al*. (2010) and Nordén *et al*. (2010). The Kłos *et al*. (2014) review of hydrology of objects in the SR-Site assessment is also used together with the interpretation of hydrology sketched by Kłos & Wörman (2013a).

Chapter 2 of this report sets out the requirements for the GEMA-Site model. Chapters 3 and 4 describe, respectively, the features of the future landscape and conceptual description of GEMA-Site. Results for a simple interpretation of the evolving system are given in Chapter 5 and an analysis of model sensitivity is given in Chapter 6. Project conclusions are found in Chapter 7.

2. Requirements

2.1. SSM's independent modelling capability

The Swedish Radiation Safety Authority (SSM) reviews the Swedish Nuclear Fuel Company's (SKB) applications under the Act on Nuclear Activities (SFS 1984:3) for the construction and operation of a repository for spent nuclear fuel. Since 2004 an independent modelling capability has been progressively developed in order to provide numerical reviews of dose assessment results. The modelling framework is known as GEMA – the generic ecosystem modelling approach and this has been used to review several assessments during this time (Kłos, 2008; Xu *et al*., 2008).

SKB has conducted a detailed site investigation programme that has been used to characterise the site and the surface environment (SKB, 2008). The biosphere component of this formed the basis for the dose assessment modelling reported by Avila *et al*. (2010). The interpretation of the site-descriptive material in SR-Site has been reviewed by Kłos *et al*. (2014) and the database for SR-Site (including Nordén *et al*. 2010) has been used to construct the model "GEMA-Site", developed to enable a numerical review of the modelling assumptions in the Avila *et al*. model.

SKB's biosphere modelling for SR-Site has similarly been developed over the past decade to incorporate increasing site specific detail. As a result the modelling approach differs from the relatively simple and robust formulation of the "reference biospheres" modelling approach. The particular features, events and processes influencing the future of the Forsmark site are set out below.

2.2. Site specificity

The degree of site specificity included in an assessment model clearly depends on the site descriptive database. SKB (2008) provides details of the likely evolution (based on the historical record and successionary evidence from the landscape to the southwest). Details from the SKB (2008) database as well as the SR-Site database (Avila *et al*., 2010; Nordén *et al*., 2010) have been made available to SSM for use in modelling. Figure 1 illustrates the approximate landscape of the land emerged from the Öregrundsgrepen over the next 5 kyear.

This is the background to the modelling carried out in SR-Site. The landscape covers an area in excess of 150 km^2. Within the landscape the geology of soils and sediments, ecosystems and hydrogeology are combined to describe the drivers of radionuclide flow, transport and accumulation in the Quaternary Deposits (QD). Detailed hydrological modelling has been carried out in SR-Site (Bosson *et al*., 2010) from which the model descriptions of basins in the landscape can be described.

This level of detail is somewhat removed from the traditional methods of biosphere modelling featuring exposure groups based on subsistence farming typically around a well. (See Walke, 2014 for a discussion of how the results from the application of simpler models compare to those obtained in SR-Site by Avila *et al*., 2010.) Of interest is the question: *Are there FEPs and combinations of FEPs in the real landscape that can combine to produce higher activity concentrations in the accessible environment that are not represented in traditional models or in SKB's landscape model?*

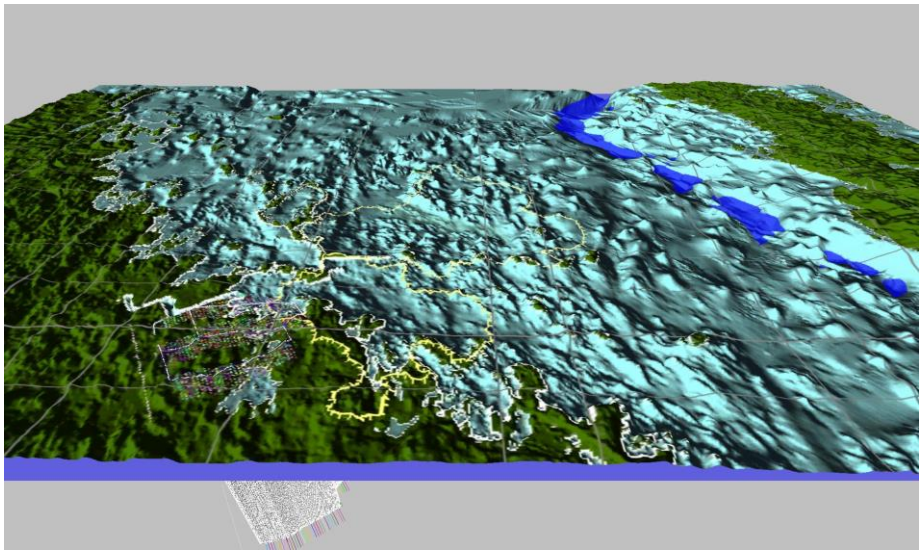

Figure 1. Landscape at 7010 CE, based on SKB's topographic map meufmhoj3085\w001001.adf. Mapped using Global Mapper 12 (www.globalmapper.com). Sea level 30 m below that of the status at 2010 CE. Approximate location of the disposal facility is indicated by the projection of the deposition holes at the surface. Land above sea level at 2010 CE is shown in green and cyan denotes emergent land areas as a result of land rise (at 6 mm year^{-1}). Two basins are shown to the northeast of the 2010 CE coastline. Beyond, to the northeast, a sequence of deep lakes are shown as the remnant of the Baltic Sea than once covered the area. Data taken from the Forsmark site descriptive modelling described by SKB (2008). The grid shows areas of 1 km^2.

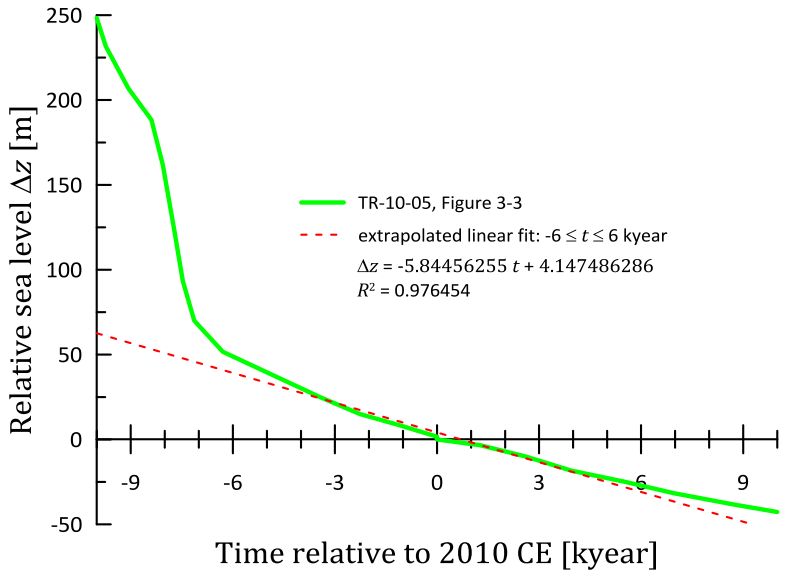

Figure 2. Shoreline displacement from 10 kyear BP to 10 kyear AP. Data interpreted from Figure 3-3 of Lindborg (2010). The fitted line to the displacement between -6 and +6 kyear is shown. The gradient is close to 6 mm year^{-1}. This forms the basis for the evolving landscape interpretation in GEMA-Site.

Using a relatively traditional modelling approach Kłos *et al*. (2011) and Kłos and Wörman (2013b) have shown that the accumulation in natural ecosystems followed by exposure in agricultural ecosystems can lead to higher consequences depending on the time allowed for accumulation before conversion to agriculture. Attention then focuses on the FEPs leading to accumulation and the timing of the change to agriculture.

Aside from the larger spatial scale of the modelling carried out in SR-Site, compared to traditional reference biosphere models, the main feature is the rapid evolution of the site. Not only is land rise an essential feature of the system than needs to be accounted since new land is emerging from the Baltic; the influence that the change in sea level has on the hydrology of the basins and catchments in the landscape is also essential. The following two sections deal with these issues in turn.

2.3. System change

Climate change is the driver of the evolution of the Scandinavian Peninsula (SKB, 2010). At the peak of the latest glacial maximum ice cover at the site is estimated to have been almost 3 km and the crustal depression caused by this loading resulted in the region being submerged by the Baltic following deglaciation. With the load removed the land has been rising, as shown in the plot of shoreline displacement as a function of time in Figure 2. These data are interpreted from Lindborg (2010) to illustrate the legacy of ice-loading and its removal caused by global warming at the end of the previous glacial episode around 10 – 15 kyear BP. Land rise from -6 to + 6 kyear can be approximated by a rate of around 6 mm $year^{-1}$ as used by Avila *et al*. (2010) in the SR-Site dose assessment modelling.

As indicated in Figure 1 the topography of the Öregrundsgrepen bed and hence future landscape is relatively flat. It is similar to that inland to the southwest of the Forsmark site. SKB therefore use the basins in the current terrestrial landscape as templates for those anticipated in the emerging landscape. Travelling inland, southwest, from the coast therefore provides a successionary journey from nascent terrestrial ecosystems to fully developed lake, wetland and forest ecosystems. As well as this natural landscape there are towns and habitations with areas of agricultural ecosystems mixed in with natural ecosystems.

In order to model the full evolutionary history of areas of the Forsmark region there is therefore a requirement that the model incorporate system change from fully submerged to coastal bay, isolated lake, wetland and forest ecosystems. At any time during the terrestrial period the natural evolution of the site may be perturbed by human actions, most importantly for dose assessments the conversion of suitable land areas to agriculture. Traditionally this has been on the relatively flat and fertile lake bed areas at the centre of the hydrologic basins (Jansson *et al*., 2006). Extensive ditching is required to convert the natural state – wetland ecosystems – into soils suitable for agriculture. There are therefore numerous changes in thickness, composition, geochemistry and water content that must be accounted in the model of the evolving system. Whereas many of these parameters can be derived from observations (Nordén *et al*., 2010; Lindborg, 2010) it is the changes to the hydrology of the basins that can be expected to have the greatest influence on the fate of radionuclides released from fractures in the bedrock.

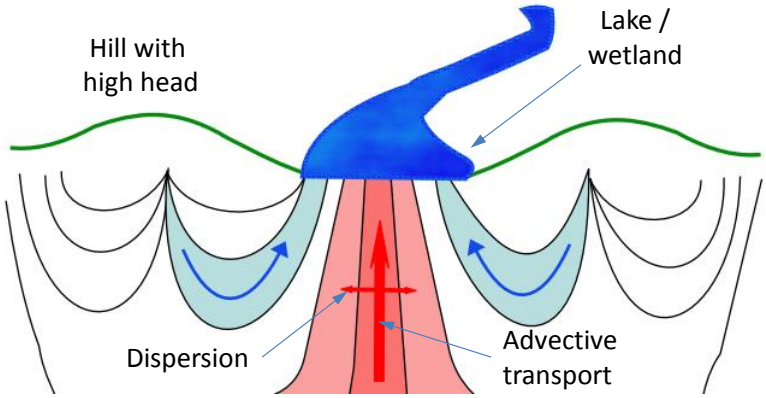

Figure 3: Schematic of groundwater discharge from large depths to surface water systems. Because the surface water system is generally located in local topographic minima the relative symmetry in the groundwater flow implies that local flow cells discharge from each side into the near-shore bottoms of the surface water, whereas deeper and more large-scale groundwater flows discharge more or less vertically into central parts of the bottom following a converging stream tube. (Taken from Kłos & Wörman 2013a).

2.4. Hydrology

Radionuclides enter the surface system of the biosphere primarily in solution in groundwaters than have been in contact with releases from the surroundings of the disposal facility. Water fluxes are therefore the primary driver of radionuclide transport and accumulation.

The bedrock is fractured and these form natural conduits that allow groundwater flows – under this influence of the regional pressure distribution – to reach the top of the bedrock. In general the volumetric flow of contaminated groundwater discharged to the Quaternary Deposits is expected to be low compared to the total circulation in the regolith. Because of the degraded structural integrity of the bedrock surrounding the fractures these locations are more susceptible to erosion and are therefore commonly found at lower elevations in the landscape. Higher elevations therefore form catchment boundaries, as illustrated by the yellow lines on the map in Figure 1.

Kłos & Wörman (2013a) sketched water fluxes in the QD for a typical basin (see Figure 3). Most of the circulation in the QD is derived from the net precipitation to the catchment area. This circulates mainly at higher elevations with gradually reducing flows at deeper levels. Discharge from the bedrock is usually at the lower parts of the basin. Although the fluxes direct from the bedrock are small in comparison to the total water flows in the basin, the circulation illustrated in the sketch focuses the captured net infiltration towards the centre of the basin where it can enhance the upward flux entering at the base of the QD, thereby boosting the upward migration of any contaminants entering the regolith from below.

The approach used for dose assessment in SR-Site takes the detailed modelling of the hydrology of six lakes in the present-day terrestrial landscape and from these derives an average circulation pattern which is then used as a template for all future

objects (see Chapter 2 of Kłos *et al*., 2014, reviewing Avila *et al*., 2010). The GEMA-Site approach is to work with the understanding of the hydrological conditions in a "typical basin" and to use this conceptual model to derive fluxes in the basin.

This document describes the initial modelling using an interpretation of the flux map described by Avila *et al*. Following the Kłos *et al*. review, requests for further information were forwarded to SKB with the aim of accessing the details of the water fluxes in the models of the six lakes at different times during their evolution.

2.5. Flexibility: modularisation

The situation is complicated in that the sketch in Figure 3 is a snapshot of the hydrology at a single time in the evolution of the landscape. The evolving model needs to account for the changes in the flux vectors as the basin transitions from sea bed to bay, to lake to wetland and finally agricultural land.

The approach taken in GEMA-Site is to use compartmental modelling techniques, identifying spatial domains in which the approximation of rapid equilibration of contaminant concentrations is valid. Transfers between the domains are then represented by first order linear kinetics. These issues concern the spatial resolution vertically and horizontally in the basin. Also of concern is the change of state of the compartments in time.

In order to provide a model of the system that is similar to that used in SR-Site the vertical resolution of the QD and water compartments is maintained, namely that of *Low*er regolith, *Mid*-regolith and *Upp*er regolith. When standing water is present a *Wat*er compartment is included. Features in the landscape of the basin are therefore comprised of a set of nested modules as illustrated in Figure 4. The basic module comprises a stack of Low, Mid, Up and Wat compartments. Interactions between compartments and with other modules in the system are then described in terms of the mass transfers between them, primarily via the water flux and solid material flux matrices, respectively **F** m^3 $year^{-1}$ and **M** kg $year^{-1}$. Other processes – for example diffusion – can be added as required. In this initial form only water and solid fluxes are explicitly modelled.

Taking a quasi-Lagrangian approach, the size and other physical chemical and biotic characteristics are described by their numerical values and their rate of change. Transfer rates between compartments *i* and *j* are given by

$$\lambda_{ij} = \frac{1}{l_i A_i} \frac{F_{ij} + k_i M_{ij}}{\theta_i + (1-\varepsilon_i)\rho_i k_i} + \frac{\dot{l}_{ij}}{l_i} + \frac{\dot{A}_{ij}}{A_i} \qquad (1)$$

where

l_i	m	thickness of the compartment,
$\dot{l}_{ij}$	m $year^{-1}$	thickness of *i* transferred to *j* in unit time
A_i	m^2	surface area of compartment,
$\dot{A}_{ij}$	m^2 $year^{-1}$	portion of surface are of *i* transferred to *j* in unit time
ε_i	-	porosity of solid material in the compartment,

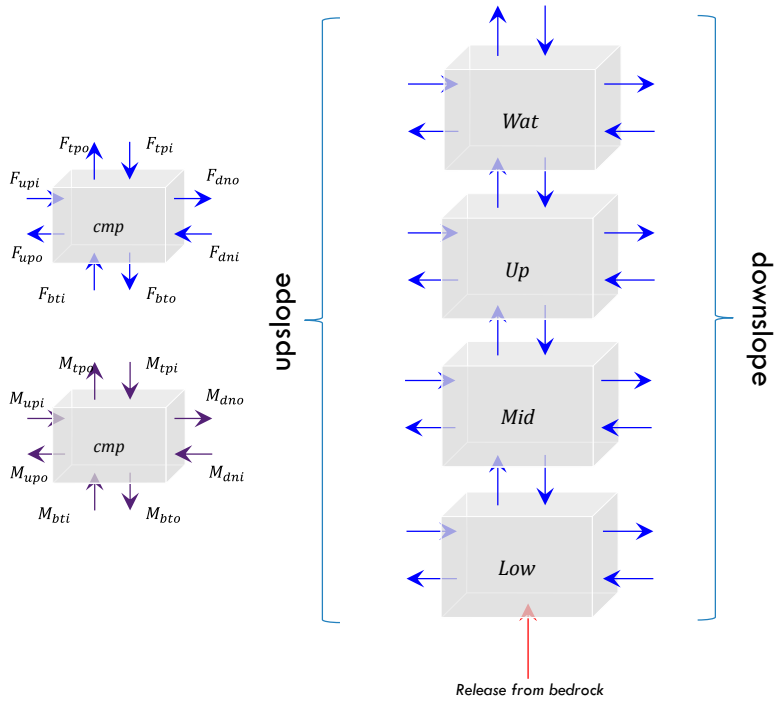

Figure 4: Modular structures of the radionuclide transport model in GEMA-Site. Each compartment in the model has interactions via up- and downslope faces as well as top and bottom faces. The components of the water and solid flux matrices are shown. These combined transfers (see Equation 1) link the compartments of each module and express fluxes into and out of the combined biosphere module. Application of GEMA-Site takes a number of modules and combines them using the lateral spatial discretisation of the system. Input (*i*) and output (*o*) fluxes are defined to each of the top (*tp*), bottom (*bt*), upstream (*up*) and downstream (*dn*) faces of the compartments. For example the water flux out of the top of the compartment of F_{tpo}, the solid material flux entering from the upstream face is M_{upi}, etc. These identifiers are used internally to ensure mass balance in the model – see Appendix 2.

θ_i	-	volumetric moisture content,
ρ_i	kg m^{-3}	density of solid material in the compartment,
k_i	m^3 kg^{-1} dw	solid – liquid distribution coefficient,
F_{ij}	m^3 year^{-1}	elements of the water flux matrix, transfers between compartments *i* and *j*, and
$\boldsymbol{M}_{ij}$	kg dw year^{-1}	elements of the solid material flux matrix.

To account for changes in time of the compartment size there are two additional terms to the inter-compartment transfer, depending on the change in compartment size that can be described as moving from *i* to *j* (compartment thicknesses and areas, respectively $\dot{l}$ m year^{-1} and $\dot{A}$ m^2 year^{-1}). In principal, each of the quantities defined in Equation 1 can be defined as an instantaneous value and its rate of change. In practice this formalism can be somewhat mitigated by the use of logical statements to control transitions (as in Avila et al., 2010). Some parameters, such as the

compartment thickness are smoothly varying functions (eg water depth as a function of isostatic uplift and sedimentation).

With this framework the characteristics of a complete basin can be integrated into the model. In the following chapter the necessary characteristics of the typical basin are discussed followed by the definition of the conceptual model and its application.

2.6. Exposure pathways

The human population of the region can interact with the potentially contaminated areas in each of the basins in many ways. Doses are evaluated for each ecosystem. To facilitate the comparison with the SR-Site LDFs (Landscape Dose Factors – SKB's indicator of radiological impact in the biosphere) the exact formulations used in Avila et al.(2010) are used. Consumption is reformulated to avoid the unnecessary reliance on carbon consumption that features in the SKB modelling. The exposure pathways calculated are:

Marine ecosystems (Sea/bay stage)	**natural ecosystems (lake/wetland/forest)**	**agricultural ecosystems**
Fish (marine)	Fish (freshwater)	berries
Crustacea (marine)	Crustacea (freshwater)	mushrooms
	water	game
	berries	external irradiation
	mushrooms	inhalation
	game	meat
	external irradiation	dairy products
	inhalation	green vegetables
		root vegetables
		cereals
		drinking water (surface, well)

The amount of consumption takes into account an autarky factor – the degree to which the area of land can support the required level of consumption. Plant concentrations are derived from both root uptake and interception of contaminated irrigation water. This latter option is not used in these initial calculations. Details of the expressions are reproduced in Appendix 1.

As the system evolves, the combination of exposure pathways actively involved changes. Marine pathways are only possible during the sea stage. Freshwater fish and crustacea can supplement local foodstuffs during the lake stage. Natural foodstuffs (those available from natural ecosystems) are those that are found in terrestrialised natural ecosystems but agricultural production requires a significantly modified landscape. It is also possible, at this stage of the evolution, for the other "natural" foodstuffs, berries, mushrooms and game, to be derived from the agricultural system.

Drinking water for humans and livestock is assumed to be obtained from the lake during this stage. As an agricultural area, the model allows water from the surface drainage system or a regolith (ie, shallow) well. Drinking water from uncontaminated (external) supplies is also allowed.

3. Example system

3.1. Future of the Öregrundsgrepen

Avila *et al*. (2010) provide a description of the marine parts of the Öregrundsgrepen, describing it as "a funnel-shaped bay of the Bothnian Sea which is a part of the Baltic Sea with its wide end to the north and the narrow end southwards". SKB have produced a digital elevation model (DEM) for the region and this DEM is used to identify 28 sub-basins in the future landscape, based on the bathymetry of the present-day Öregrundsgrepen. The basins identified by SKB are illustrated in Figure 5.

Avila *et al*., (2010) also note that:

> The small-scale topography of the area gives rise to many small catchments with local, shallow groundwater flow systems in the regolith. In combination with the decreasing hydraulic conductivity with regolith depth, this causes that a dominant part of the near-surface groundwater will move along shallow flow paths. Shallow groundwater flow paths imply strong interactions among evapotranspiration, soil moisture content, groundwater levels and flow. In Forsmark, the groundwater table in the regolith is very shallow; in general the depth to the groundwater table is less than a metre. Thus, the groundwater level in the regolith is highly correlated with the topography of the ground surface. This local flow system in the regolith overlies a larger-scale flow system in the bedrock.

Each of the basins can be treated as independent from the others in the hydrological modelling (Bosson *et al*., 2010). In this way, SKB use a combination of detailed modelling MIKE-SHE of representative lakes in the present-day terrestrial biosphere to derive a snapshot of the hydrological characteristics of what they term an "average object". They further use MIKE-SHE to determine the locations of potential release locations in the future landscape, (see Lindborg, 2010).

3.2. Key features of a typical basin

The development and implementation of the GEMA-Site model requires a representative landscape object. The intention is to use a generic Forsmark basin as a first step towards a more detailed model. Avila *et al*. (2010) describe the basins as "lake-centred catchments. For reference, therefore, Basin 116 is selected. As shown in Figure 5, a well-defined lake is expected to develop over the next few millennia and there are several potential release locations associated with it. Although this is not the object in the SKB landscape model that gives rise to the highest landscape dose factors, it does contain all the features necessary for the GEMA-Site implementation.

Figure 6 illustrates Basin 116 with a cross-section between the catchment boundaries. This is the representative basin that will be used in subsequent chapters to illustrate the development of the GEMA-Site model.

As can be seen from the profile, there is a general trend of decreasing elevation to the northeast with the bed of the future lake clearly identifiable in the centre. The shaded area on the map represents the location of the lake based on the current bathymetry. As see level falls different parts of the basin will emerge at different times and the succession of ecosystem will begin.

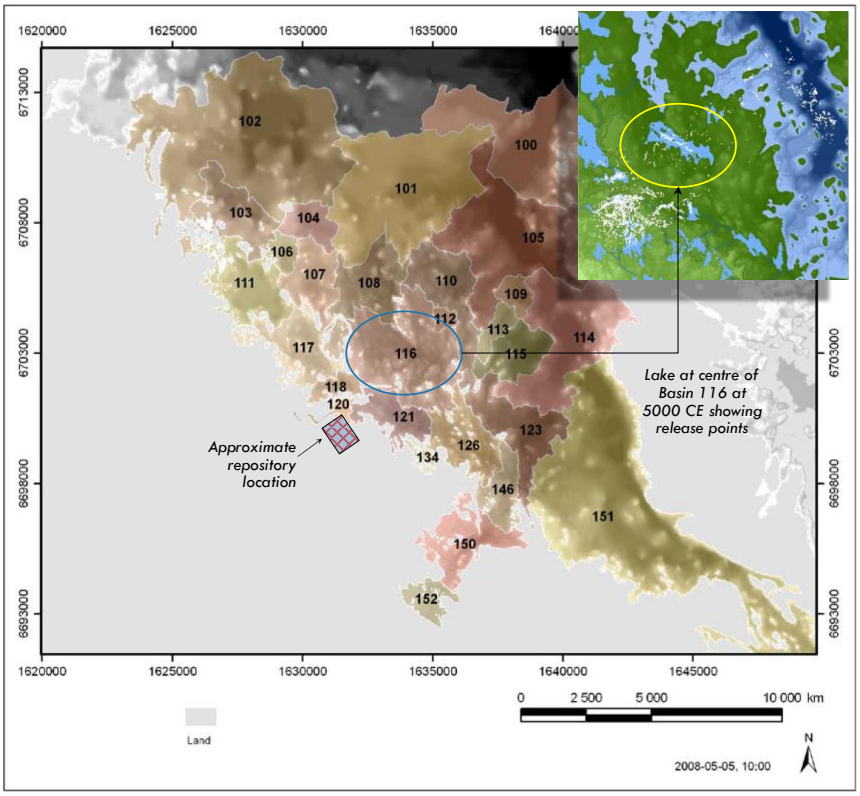

Figure 5: Sub-basins in the Öregrundsgrepen basin, based on present day bathymetry. (Reproduction of Figure 2-2 of Avila et al., 2010). SKB identify basins by a numeric code. Inset is a map from Lindborg (2010) showing all calculated release points (white dots) in the landscape. The selected object is a lake at the centre of Basin 116 at 5000 CE.

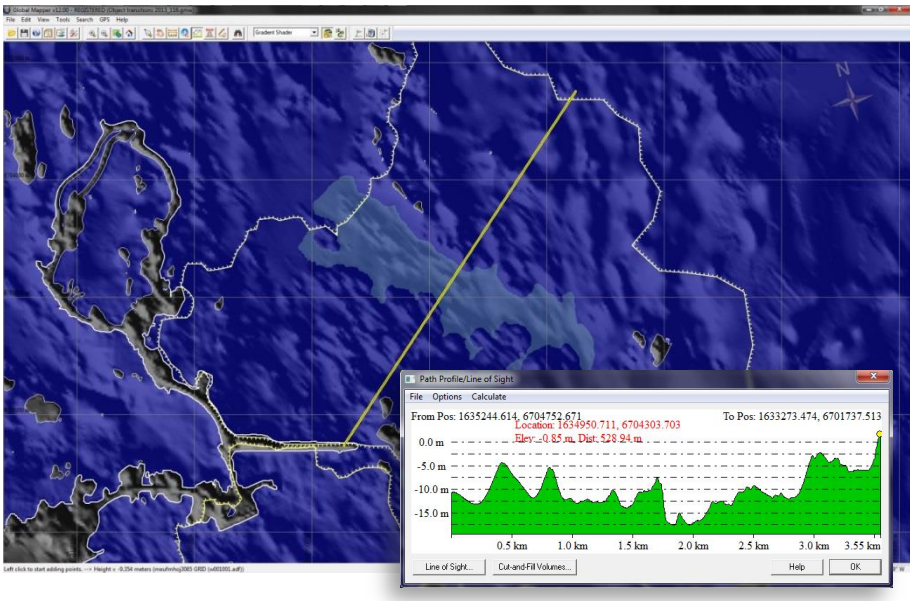

Figure 6: Object 116 in the future Forsmark landscape. Map drawn using Global Mapper 12 with the topographic data set provided by SKB. The depth profile shown runs from NE to SW. The basin boundary is indicated and the area of the future lake/wetland is shaded at the deeper part of the basin. Depths are representative of the situation at 2000 CE.

SKB's map of potential release locations to the area depicted in Figure 5 shows that the releases are focused on the centre of the future lake (see chapter 6 of TR-10-05; Lindborg, 2010). This is the deepest part of the basin and corresponds, approximately, to the locations of lineaments in the bedrock (Lindborg, 2010). How this is represented in GEMA-Site is discussed in the next Chapter.

4. Conceptual model for the evolution of the basin

4.1. System identification and justification

Figure 6 illustrates a typical basin in the Forsmark landscape and Figure 3 is a sketch of how deep groundwater mixes with the infiltration over the catchment. The task in GEMA-Site is to capture the concept in Figure 3 in the context of the basin in Figure 6. Clearly some approximation is required in respect of the spatial structures in the basin as well as how the flux vectors in the Quaternary Deposits change as the landscape evolves.

Because the lake is at the centre of the catchment with release to the lowest part of the terrain, the situation of the basin as terrestrial ecosystems with a lake at the centre is first considered as a snapshot. This interpretation is then generalised to consider the state of the basin and hydrology at different snapshots during the evolution.

In the basin three areas can be distinguished, using the SKB terminology from Avila et al. (2010):

- The water body area – "the lake" - A_{aqu}
- The terrestrial area surrounding the lake - A_{ter}
- Subcatchment area, ie the area outside the lake/wetland system- $A_{SubCatch}$.

Avila *et al*. also assume three distinct layers in the QD, namely lower, mid and upper regolith. Together with a standing water layer, these can be used to identify the water fluxes in the near surface hydrology. Overall the juxtaposition of components in the model suggests a cylindrical geometry, as shown in Figure 7. The water fluxes illustrated in the figure can readily be linked to the modular fluxes shown in Figure 4. The modularisation also suggests that Figure 4's basic structure can be used to represent the areas in the basin. For the subcatchment and terrestrial areas three compartments can be used, with no standing water compartment. For the aquatic area the water compartment is active.

4.2. Spatiotemporal discretisation

While Figure 7 illustrates one stage during the evolution of the basin, similar to that used in describing the "average object" in SKBs interpretation of the site (Bosson *et al*., 2010) it should be appreciated that it is just a snapshot. In order to represent the distribution of radionuclides entering the basin as it evolves, a representation of the changing conditions in different parts of the structure is necessary.

Figure 8 illustrates how stages in the evolution affect the spatiotemporal discretisation in relation to the topography of the basin. From the transect illustrated in Figure 6, a low spatial resolution profile can be proposed, as shown. In this development of the initial version of GEMA-Site three parts of the basin are identified:

- Outer basin (*Outer*)
- Inner basin (*Inner*), and
- Central basin (*Central*)

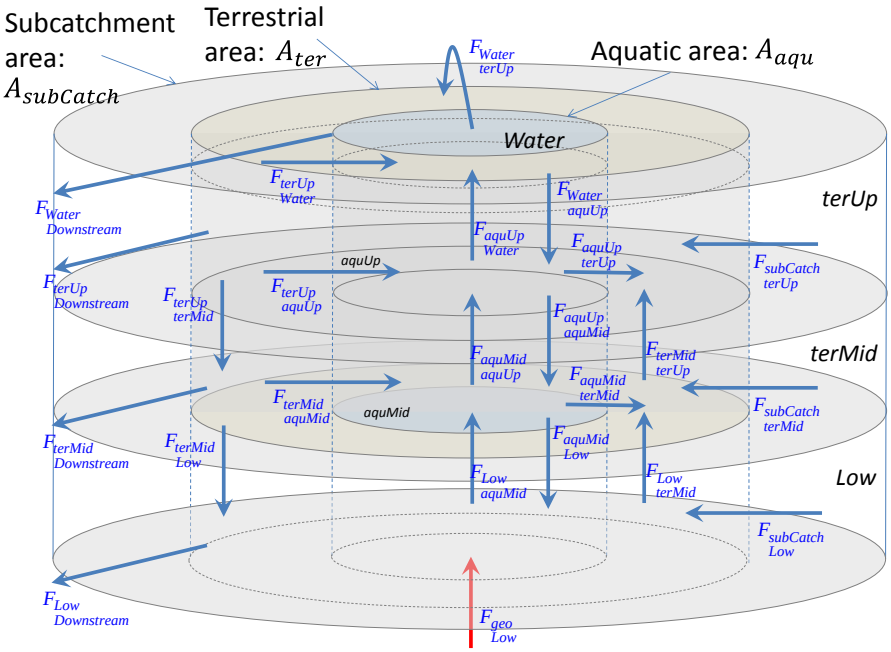

Figure 7: Interpretation of areas and boundaries for a lake-centred catchment. Arrows indicate water fluxes (m^3 $year^{-1}$) required to characterise transport and accumulation. The three domains of aquatic, terrestrial and uncontaminated sub-catchment are distinguished.

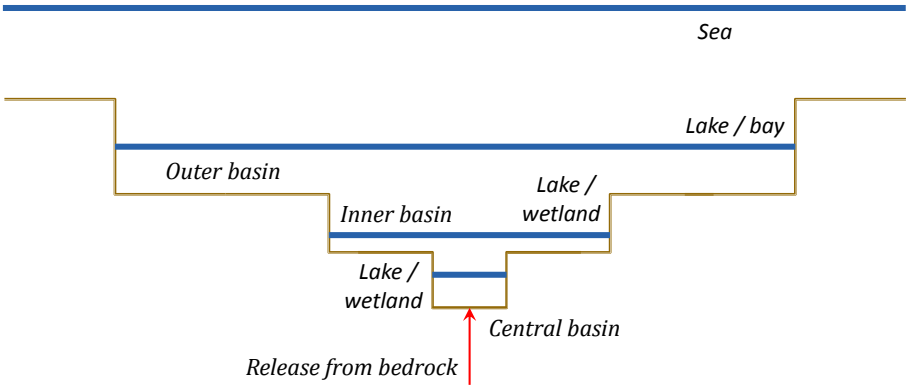

Figure 8: Topography and spatial discretisation of the basin in GEMA-Site. At early times there is complete water cover for the basin – this is the sea stage. As land rises the outer basin emerges (bay/lake stage). Further land rise (and sedimentation) causes the water columns to be confined to the inner basin (lake/wetland stage) and subsequently the inner basin is a wetland and the lake in the central basin. Ultimately the basin drains through a small water body situated in the centre of the basin. Agriculture is possible at any stage in any module where there is a land surface, though attention here focusses on agriculture in the central basin only..

Clearly a higher lateral resolution is possible and may be required, depending on the assessment context. For this stage of development, however, three discrete areas suffice to illustrate the principle. The modularisation of the model described in Section 2.5 is designed to allow the practical inclusion of additional spatial discretisation. A coarse representation would have a single object (the whole basin). At a higher spatial resolution, two modules can represent the outer and inner parts (similar to SKB's subcatchment + object); with three modules the outer, inner and central basin are distinguished (subcatchment + terrestrial and aquatic objects) and so on.

Figure 8 also shows the local "sea level" at different stages in the evolution. This interpretation can be used to identify different temporal domains in the model. Initially the whole basin is covered by sea and this lasts until the end of the "sea stage" at time t_{sea} [year]. After this stage the landscape forms a bay which gradually contracts to form an isolated lake. This transition occurs at time t_{aqu}. After this the area is in a natural state (ie, uninfluenced by human action) and natural ecosystems continue to develop. The time taken for terrestrial species to colonise the emergent land area is denoted by t_{colony}. Human action can radically alter the conditions within the modules. For this reason one more timing event is included: t_{agri} is the time at which agricultural ecosystems are imposed within the object by human activity.

In practice, transitions in each of the modules identified in Figure 8 can be controlled in the model using these parameters. Avila et al. (2010) employ a similar set of "threshold" times to govern changes in the SKB implementation.

Transfers of radionuclides between the spatial domains of each of the modules are described by Equation (1) on page 7. The subscript *i* denotes the position of the compartment in the network representing the spatial discretisation of the basin. These take the values

- *Wat* – surface water compartment
- *Up* – upper regolith
- *Mid* – mid-regolith
- *Low* – lower regolith

Each of the parameters in Equation (1) can then be linked to data values representative of the site (cf. Nordén *et al*., 2010 as interpreted by Avila *et al*., 2010). In this formalism it is also useful to denote the module associated with each of the parameters. In this way $t_{sea} \rightarrow \left[t_{sea}^{Outer}, t_{sea}^{Inner}, t_{sea}^{Central} \right]$, and so on for all necessary modules in the spatial discretisation.

Equation (1) includes only two spatial translations, namely the water and solid material flux vectors **F** and **M**, the components of which are shown in Figure 4 in relation to each of the faces of the nominal Cartesian compartments structure, namely the inputs and outputs across the faces:

- upstream – *upi, upo*
- downstream - *dni, dno*
- top – *tpi, tpo*; and
- bottom – *bti, bto.*

Mass balance in the model can therefore be ensured by matching the outputs from one compartment to the inputs to the adjacent. The example of the model implemented here is listed in Appendix 2.

4.3. Fate of radionuclides in the basin: a narrative

The fate of radionuclides entering the basin can be explained by developing the interpretation of hydrology shown in Figure 3. Figure 9 illustrates five stages in the development of the three-module model described previously. Release to the basin is from the bedrock fracture at the deepest part of the regolith in the basin (red arrow). There is a small advective pressure from the fracture driving contaminated groundwater from the bedrock into the sediments above the crystalline bedrock.

During the **sea stage** of the basin's development ($t < t_{aqu}^{Outer}$) this small flux, entering the lower regolith of the central basin, is assumed to continue up through the sedimentary material on top of the bedrock, ultimately discharging to the water column of the Central basin. Most of the advective fluxes in the basin are determined by bulk water movements in the Öregrundsgrepen, moving the contents of the water compartments laterally. This is modelled by Avila *et al*. in terms of the residence time of packets of water in the water column. This approach is also adopted here. There is a relatively small exchange of water with the atmosphere via precipitation and evaporation.

In reality it may be anticipated that the discharge of water from the bedrock, entering the lower regolith, may not reach the water column and that there is considerable dispersion within the intervening regolith layers. Mixing within the lower regolith and other layers is, of course, part of the way in which the spatial domain of the compartment is defined. Diffusive processes within the regolith compartments can also be expected to disperse radionuclides laterally. In this initial version of GEMA-Site, however, diffusive processes are not represented although they are in the Avila *et al*. model.

Consequently only the advective flux is represented in the model, causing an upward transport of contaminants from the fracture in the bedrock. Activity entering the base of the lower regolith is therefore transported upwards through the mid- and upper regolith, entering the water column where it is rapidly dispersed into the wider sea. Sorption onto solid material in the water column can lead to the transfer of activity to the upper regolith of the inner and outer basins (and thence deeper into the regolith should bioturbation and diffusion be active). The net result of release during the sea stage is therefore to accumulate activity in the lower regolith of the central basin, the mid and upper regolith layers of the central basin and the water column. Low concentrations in the water columns in each of the modules disperses small fractions of the total inventory to the regolith in the whole basin.

By the **bay/lake stage** ($t < t_{aqu}^{Inner}$) there is a small residual inventory in the upper regolith of the outer basin, from where the water column has disappeared as a result of land rise. In the outer basin there is a net infiltration through the upper regolith. Some of the infiltration moves vertically to the mid-regolith, some moves to the adjacent upper regolith of the inner basin. A similar pattern is assumed in the mid-regolith, with transfers to the lower regolith and the mid-regolith of the inner basin. In the lower regolith the transfer is assumed to be constrained to the inner basin's lower regolith. This is a no-flow boundary condition at the lower surface.

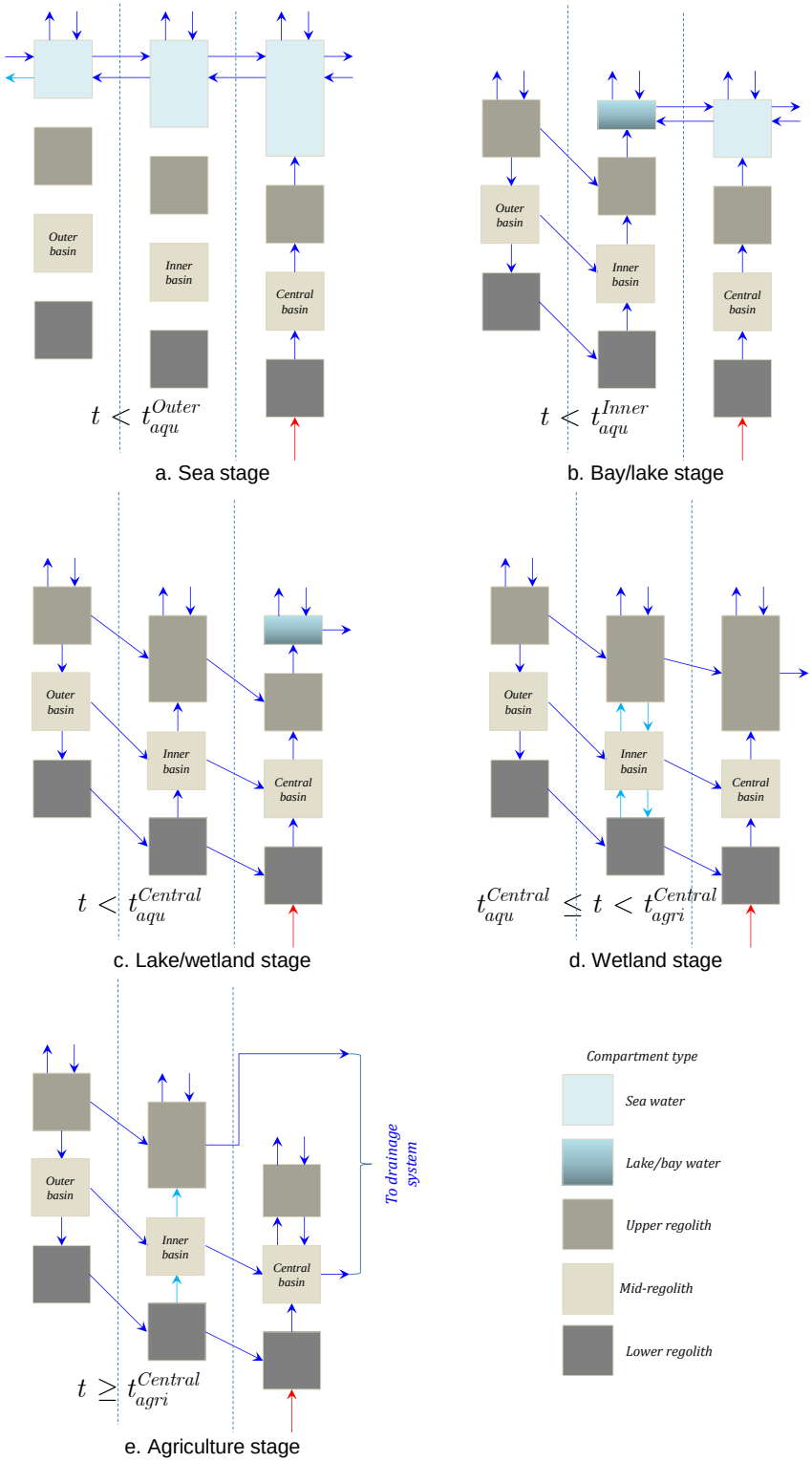

Figure 9: Evolution of hydrology during land uplift. Outer, inner and central basins are shown from left to right. With uplift and sedimentation the water level drops in each module. Release is to the lowest part of the basin with a small upward flux at all times. As water levels fall, flow from the outer, then inner basin is directed sub-horizontally towards the central basin contributing to increased upward fluxes. Change to agricultural conditions necessitates a modified and maintained drainage system.

In the inner basin there is now the possibility of an upward flux through the regolith layers to the water column of the bay/lake. This is driven by the flux from the outer basin. As with the distribution of the water fluxes in the outer basin, there is the potential for flow from the regolith layers in the inner basin to those in the central basin. The focussing towards the central basin of net infiltration captured in the outer basin contributes to enhanced upward fluxes through the regolith of the inner and central basins. There is exchange of water in the water columns of the inner and central basins and there is a loss from the water of the central basin that is still in direct contact with the remaining Öregrundsgrepen. During this period the thickness of the upper regolith in the inner basin also increases as a result of sedimentation.

By the **lake/wetland stage** ($t < t_{aqu}^{Central}$), the lake provides the downstream outlet for the basin. This is in the central basin and there is surrounding wetland that has accumulated upper regolith material during the lake/bay phase of the inner basin. The outer basin – at higher elevations – is likely to consist of forest ecosystems that have colonised the emergent land surface, with a thin layer of upper regolith compared to the inner and central basins where there are greater accumulations of sediment.

At this stage of development the intercepted net precipitation in the outer basin is again directed downwards and inwards towards the lower parts of the basin. Potentially there is still a small upward flux in the inner basin. As before there is an increased flux entering the domain of the central basin, allowing for the increased overall water flux due to the captured infiltration. A precise map of the distribution of the fluxes requires sophisticated modelling (cf. Bosson *et al*., 2010) but there will be increased upward flux from the lower to mid- to upper regolith in the central basin, acting to drive any accumulation of radionuclides at the interface between the bedrock and the regolith upwards. During this phase there is ongoing accumulation in the upper regolith of the central basin and the depth of the water column in the central basin is decreasing due to uplift and sedimentation.

Radionuclides may continue to enter at the base of the central basin and move upwards due to the bedrock-to-lower regolith flux. The upward flux at the top of the lower regolith is increased due to the contribution of the captured infiltration entering from the sides of the lower regolith in the inner basin. In addition to the radionuclide flux from the bedrock, any (albeit small) accumulations in the compartments of the outer and inner basins will circulate with the water fluxes around the compartments of the modules in the basin.

In this three module representation of the basin, the final stage of *natural* evolution is the pure **wetland stage** ($t_{aqu}^{Central} \leq t < t_{agri}^{Central}$). The water table remains close to the surface, especially in the inner and central basins. As interpreted here this means that what loss there is from the basin is from drainage of the upper regolith in the central basin. There may be semi-permanent streams during this period. A more complete model of the basin would include these explicitly. Again, the most important issue for the model is the representation of flux vectors between the regolith layers of the outer, inner and central basins. The loss from the central basin must take into account all inputs (across the geosphere-biosphere interface plus intercepted infiltration from outer, inner and central modules).

Overall, the fate of radionuclides entering the basin is to circulate from the lower regolith of the entry point. If there is little retention (weakly sorbing species) there will be significant loss from the system. Nevertheless there will be recirculation around the basin. More strongly sorbed radionuclides will be retained at deeper levels. The increased flux in the lower regolith of the central basin occasioned by the

capture of relatively large volumes of infiltration in the inner and outer basins will act to accumulate activity in the upper regolith of the central basin. Kłos and Wörman (2013a) and Kłos *et al*. (2011) have shown the potential importance of high accumulation in natural ecosystem prior to conversion to agriculture.

The **agricultural stage** ($t \geq t_{agri}^{Central}$), has a drainage system imposed on the natural landscape's drainage by the human population. As shown only the central basin is assumed to be used for agriculture. In principle though, any of the modules could be converted at time $t = t_{agri}^{module}$, for *module* = Outer, Inner, Central. In this case, the large combined volumetric flow from the outer and inner basins that would enter the upper regolith of the central basin is diverted in excavated ditches so as to bypass the central area. Drains are also emplaced in the mid-regolith of the central basin so as to prevent the net infiltration in the central basin from saturating the agricultural soils. There is residual flow from the mid- and lower regolith layers in the inner and outer basins. NB, this interpretation does not account for irrigation, which is modelled, as required, as an abstraction with interception by the crop before flowing to the upper regolith.

The key to the model is therefore understanding water inputs and losses from the basin and understanding the internal variation in time and space of the water flux vectors between the different regolith layers. Chapter 5 of this report interprets the basic lake/wetland snapshot (the "average object" from Bosson *et al*., 2010) as used in the Avila *et al*. (2010) modelling for SR-Site.

5. Application: region specific basin

5.1. System description

5.1.1. Basin characteristics

The GEMA-Site model focusses on interpretation of the hydrology in the basin. Water fluxes in the basin are overwhelmingly dictated by the infiltration of captured precipitation. In other words, the hydrology is determined by the size of the catchment and the physical characteristics of the material in the basin. The model is implemented in Ecolego (Facilia, 2013).

Table 1 lists the numerical values of the region specific characteristics of the model. These include the regional precipitation (P m year^{-1}) and evapotranspiration (E m year^{-1}) as well as the assumed values for the advective velocity of water entering at the base of the lower regolith, carrying with it radionuclides in solution. SKB distinguish release from the bedrock under marine and terrestrial conditions (Bosson *et al*., 2010) but there is some question of interpretation (see Section 5.1.3 below). The release flux during the sea stage is set to $v_{geo,sea} = v_{geo,ter}$ = 0.01 m year^{-1}. A constant land uplift rate is assumed over the period of the modelling, derived from Figure 2.

The total volumetric throughput is determined by the areas of the different modules in the basin. Table 2 lists the areas in the Avila et al. model for the objects shown in Figure 5. Taking Object 116 as reference in the definition of the GEMA-Site model is helpful in the sense that the averaged areas are similar. The mean basin size over the whole landscape is 10^7 m^2 with the "lake"[1] being 8.5×10^5 m^2. Object 116 has a basin area of 1.4×10^7 m^2 and a "lake" area of 1.6×10^6 m^2.

In the GEMA-Site interpretation the three modules are identified as follows:

- **Outer basin** – taken to be the overall size of the basin (implicitly less the area of the inner basin). For initial modelling purposes, therefore A_0^{Outer} = 10^7 m^2.
- **Inner basin** – the maximum lake area (less the area of the central basin). A_0^{Inner} = 10^6 m^2.
- **Central basin** – there is no specific information from the SKB database on the dimension of this part of the basin. The profile in Figure 6 is useful in this respect. A value of $A_0^{Central}$ = 10^5 m^2 is used for these initial modelling purposes.

Table 3 summarises the characteristics of the three GEMA-Site modules.

[1] SKB have a fixed size for the lake and wetland combined in their modelling. This area is the maximum extent of the lake and wetland. In GEMA-Site, with the three module spatial discretisation, the area with standing water – the lake – changes in size during the evolution. The size of the lake denoted by Lindborg (2010) is therefore the area of the depression in the basin around which the highest closed contour can be drawn. Above this level there is contact with the sea. This approach is used in Figure 6 to identify the location of the lake in basin 116 in the GEMA-Site definition. This area is identified as the area of the *inner basin*.

Table 1: Region specific details for the implementation of GEMA-Site described here.

Parameter		Value	Module	Description
P	m year^{-1}	0.56	all basin	Precipitation (Lindborg, 2010)
E	m year^{-1}	0.4	all basin	Evapotranspiration (Lindborg (2010)
$v_{geo,sea}$	m year^{-1}	0.01	all basin	Bedrock adv. velocity sea stage (Bosson *et al.*, 2010). Central basin only.
$v_{geo,ter}$	m year^{-1}	0.01	all basin	Bedrock adv. velocity non-sea stage (Bosson *et al.*, 2010). Central basin only.
τ_{wat}	year^{-1}	0.017	All basin	Residence time of water parcels in grepen (Aquilonius, 2010)
$\dot{l}_{uplift}$	m year^{-1}	-0.006	all basin	Isostatic uplift rate, interpreted from SKB(2010), see Figure 2

Table 2: Catchment areas of objects in the SR-Site landscape model. Data taken from Table 7-5 of Lindborg (2010), quoting data from Löfgren (2010). Object 121 is modelled as three distinct areas with a lake in only one of them. The date at which the land first emerges from the Baltic and the time at which the sea is finally absent are shown. Object 116 is emphasised.

SR-Site object	basin area m^2	lake area m^2	First land CE	Last Sea CE
101	2.18E+07	3.36E+05	1997	8015
105	3.56E+07	1.36E+06	798	11,156
107	4.84E+06	1.43E+06	669	3497
108	7.58E+06	1.42E+06	767	5011
114	2.63E+07	2.66E+06	-1185	8545
116	1.41E+07	1.60E+06	757	4783
117	1.61E+07	1.87E+06	-1347	2997
118	2.00E+06	3.60E+05	287	2848
120	1.03E+07	3.01E+05	-1725	2409
121_1	3.56E+06	2.38E+05	486	4007
121_2	8.92E+05		876	2865
121_3	6.38E+05		765	3620
123	7.71E+06	4.66E+05	261	6482
124	2.44E+05	8.27E+04	574	1888
125	4.21E+05	7.61E+04	693	1902
126	6.25E+06	5.60E+05	477	4379
136	3.59E+06	6.11E+05	53	1898
146	3.82E+06	2.42E+05	255	4748
mean	1.04E+07	8.51E+05		
max	3.56E+07	2.66E+06		
min	2.44E+05	7.61E+04		

Table 3: Numerical values used in the definition of the GEMA-Site modules for a representative basin. Values are based on a projection of land rise for the map shown in Figure 6 with land rise at 6 mm year^{-1}. See text for details.

Parameter	Units	Value	Scope	Comments
A_0	m^2	10^5	Central Basin	Initial object area
l_{bay}	m	5	Central Basin	Depth on isolation from sea
t_{colony}	year	100	Central Basin	Time for terrestrial colonisation
t_{agri}	year	19000	Central Basin	Time of conversion to agriculture
l_{min}	m	0.01	lower regolith	Minimum allowed thickness
l_0	m	1	lower regolith	Initial thickness
l_{min}	m	0.01	mid regolith	Minimum allowed thickness
l_0	m	0.9	mid regolith	Initial thickness
l_{min}	m	0.01	upper regolith	Minimum allowed thickness
l_0	m	0.1	upper regolith	Initial thickness
$l_{agri,root}$	m	0.3	upper regolith	Agricultural rooting zone
l_{min}	m	0.2	water	Depth at end of aquatic state
l_0	m	80	water	Initial water depth
A_0	m^2	10^6	Inner Basin	Initial object area
l_{bay}	m	5	Inner Basin	Depth on isolation from sea
t_{colony}	year	100	Inner Basin	Time for terrestrial colonisation
t_{agri}	year	25000	Inner Basin	Time of conversion to agriculture
l_{min}	m	0.01	lower regolith	Minimum allowed thickness
l_0	m	1	lower regolith	Initial thickness
l_{min}	m	0.01	mid regolith	Minimum allowed thickness
l_0	m	0.9	mid regolith	Initial thickness
l_{min}	m	0.01	upper regolith	Minimum allowed thickness
l_0	m	0.1	upper regolith	Initial thickness
$l_{agri,root}$	m	0.3	upper regolith	Agricultural rooting zone
l_{min}	m	0.2	water	Depth at end of aquatic state
l_0	m	75	water	Initial water depth
A_0	m^2	10^7	Outer Basin	Initial object area
l_{bay}	m	5	Outer Basin	Depth on isolation from sea
t_{colony}	year	100	Central Basin	Time for terrestrial colonisation
t_{agri}	year	25000	Outer Basin	Time of conversion to agriculture
l_{min}	m	0.01	lower regolith	Minimum allowed thickness
l_0	m	1	lower regolith	Initial thickness
l_{min}	m	0.01	mid regolith	Minimum allowed thickness
l_0	m	0.9	mid regolith	Initial thickness
l_{min}	m	0.01	upper regolith	Minimum allowed thickness
l_0	m	0.1	upper regolith	Initial thickness
$l_{agri,root}$	m	0.3	upper regolith	Agricultural rooting zone
l_{min}	m	0.2	water	Depth at end of aquatic state
l_0	m	70	water	Initial water depth

Following the example of the SR-Site modelling, GEMA-Site is setup to model the evolution of the basin from the end of the glaciation to several thousand years in the future. Initially then, the Baltic covers the entire site to a depth of several tens of metres, as in Figure 2. From Löfgren (2010) the initial depth of the central basin is taken to be 80 m and, as a simplification, each of the modules suggested by the profile in Figure 6, the mean elevation of each of the modules is taken to be 5 m higher. Therefore

- $l_0^{Central}$ = 80 m
- l_0^{Inner} = 75 m
- l_0^{Outer} = 70 m

The values therefore represent a mid-sized object with a central part of the basin 10 m deeper than the outer basin.

For each of the modules the initial and minimum thickness of compartment layers are set. The initial thicknesses are taken from the definition of the sea stage in Avila *et al*. (2010). The initial state of the regolith thicknesses are therefore the same in each module – 1m for the lower regolith, 0.9 m for the mid-regolith and 0.1 m for the upper regolith. Organic material accumulates at the surface, increasing the thickness of the upper regolith. On conversion to agricultural land this is compacted and the thickness reduced. The thickness of the rooting zone for agricultural ecosystems can be set for each module (although here only the basin is used for farming). A value of 0.3 m is assumed corresponding to the Avila *et al*. model.

The minimum thicknesses set to avoid numerical problems as the water level decreases or the media in the regolith layer is eroded. Section 5.1.2 describes the timing of events in the model in more detail.

Other numerical data for the media in the basins are described in Appendix 3 for both nuclide specific and non-specific parameters.

5.1.2. Timing parameters and evolution

At some stage during the rise of the sea bed, the water in the basin becomes isolated from the rest of the bay. The time of conversion is defined in the same way for each module, namely when the water level drops below l_{bay} = 5 m.

There are four transitions in the evolution of each module.

- t_{sea} – transition from sea to bay
- t_{aqu} – end of the aquatic period (no standing water in the module: water compartment disconnected and inventory redistributed)
- t_{colony} – the time taken for colonisation of the emerged land by terrestrial biota. A value of one hundred years is assumed
- t_{agri} – the time at which transition to agricultural conditions is imposed by the local human population. In Table 3 only the Central basin is converted to agricultural land in the modelling interval of 20 kyear, with $t_{agri}^{Central}$ = 19000 year.

The sea-bay and end of the aquatic periods are determined at run-time, depending on uplift and sedimentation. for each of the modules, therefore:

$$t_{sea} = \left| \frac{l_0 - l_{bay}}{\dot{l}_{uplift} - \left(M_{tpi} - M_{tpo}\right) / A_{obj}\rho_{gl}} \right|$$
$$t_{aqu} = t_{sea} + \left| \frac{l_{bay}}{\dot{l}_{uplift} - \left(M_{tpi} - M_{tpo}\right) / A_{obj}\rho_{peat}} \right| \quad (2)$$

During the sea stage the sediment material is assumed to be equivalent to the glacial clay that constitutes the bed of the Öregrundsgrepen. Density is of the clay is ρ_{gl}, kg m^{-3} from Lindborg (2010). The material deposited during the aquatic phase after the sea stage is similarly calculated but the density is that of peat (ρ_{peat}, kg m^{-3}) that accumulates at the bottom of Swedish lakes. Numerical values are taken from Lindborg (2010). The net sedimentation considers the balance of solid material fluxes at the top of the upper regolith compartment $M_{tpi} - M_{tpo}$, kg $year^{-1}$.

5.1.3. Water, solid material fluxes and mass balance

Equation (1) shows how transfer rates are evaluated in the model. It places a strong emphasis on the water and solid material fluxes from the i^{th} to the j^{th} compartment in the network. Practically, this means that each snapshot in Figure 9 requires a separate flux map for each module. There are then five sets of fluxes to be determined using the parameters in Table 1 and Table 3. For reference, full details from the model are given in Appendix 2. There is some repetition and not all the flux maps differ greatly between snapshots. The following provides an overview of the method as applied to part of the evolution.

During the **sea stage** the only advective flux in the regolith is that from the geosphere, therefore in the Central basin

$$F^{Central}_{low,bti} = v_{geo} A^{Central}_{obj} = F^{Central}_{low,tpo} = F^{Central}_{mid,bti} = F^{Central}_{mid,tpo} = F^{Central}_{upp,bti}$$
$$F^{Central}_{n,bto} = 0 \qquad n = low, mid, upp, wat \quad (3)$$

ie, this flux propagates upwards through the regolith column of the central basin until it enters the water compartment. There is no downward flux in the regolith or from the water compartment but there are lateral exchanges between the water column of the central basin and adjacent modules[2]:

[2] Mass balance is explicitly addressed in this model. The three terms in addition to the turnover time are an expression of this but are small in comparison with the overall exchange of volumes of water in the water column. As a consequence of mass balance being explicit, water input from outside the modelled area is included from "upstream" and "downstream" directions in the conceptual model. Transfers out of the system carry radionuclides in solution but inflows do not. Implicitly, therefore, the water volume outside the model has zero concentration.

Table 4: Summary of fluxes in the modules of the modelled basin at the different snapshots in Figure 9. Implementation is described for selected cases here. For full model implementation see Appendix 2.NB, although each part of the basin could be converted to agriculture, this interpretation assumes that only the central basin is converted during the 20 kyear period modelled.

Evolution snapshot	Module	Characteristics of the flux map
Sea (Figure 9a)	All	Described. Most water exchange in the water column. Explicit representation of bedrock driven transport in central basin regolith.
Bay/Lake (Figure 9b)	Outer	Described. Fluxes driven by net precipitation. Flux vectors interpreted as vertical and lateral components
	Inner	Described. As Sea stage with additional input from Outer basin
	Central	As sea stage.
Lake/ Wetland (Figure 9c)	Outer	As bay/lake stage
	Inner	Similar to outer basin bay/lake stage but with additional upstream inflows
	Central	Similar to Inner basin bay/lake, simplified lake water drainage
Wetland (Figure 9d)	Outer	As bay/lake
	Inner	As lake/wetland
	Central	Similar to inner basin, lake/wetland stage. Drainage from upper regolith compartment
Agriculture (Figure 9e)	Outer	As bay/lake
	Inner	As lake/wetland, upper loss to drainage not central compartment. Does not affect mass balance in inner basin
	Central	Modified, basin drainage from central mid and exchange between up-per and mid compartments

$$F_{wat,upi}^{Central} = F_{wat,upo}^{Central} = F_{wat,dni}^{Central} = F_{wat,dno}^{Central} = A_{obj}^{Central}\left(\frac{l_{wat}^{Central}}{\tau_{wat}^{Central}} - v_{geo} - P + E\right), \quad (4)$$

As indicated in Figure 9, any activity entering the central basin therefore enters the sea and is distributed throughout the system. Transfer of radionuclides to the regolith compartments of the inner and outer basins only arises as a result of sedimentation:

$$\begin{aligned} M_{wat,bto}^{m} &= M_{upp,tpi}^{m} = s_{ned} \\ M_{upp,tpo}^{m} &= M_{wat,bti}^{m} = s_{upp} \\ m &= Inner, Outer \end{aligned} \quad (5)$$

The two opposing rates of deposition and resuspension, respectively s_{ned} and s_{upp} are taken from the Avila *et al*. modelling using average numerical values for Object 116 obtained from the time series Excel workbook ParametersTS.xlsx provided to SSM by SKB in 2012 (SKB, 2012). These are assumed to be in balance as modelled in this initial implementation.

No other solid material transfers are included – there could be transport of suspended solid material between and, externally, to the water column in the basin but this is not assumed here. Similarly there may be bioturbation in the regolith compartments of the bed of the bay but the overall radionuclide transfers can be expected to be small. This implementation focuses on advection-driven transfers. The result is that there is an accumulation in the regolith of the central basin, low concentrations in the water column of the whole basin and a small accumulation in the upper regolith of the bay bed sediment. Any radionuclide reaching the water compartments will be rapidly dispersed in sea water.

As land rises, the outer basin emerges from beneath the waves. During this **bay/lake stage** processes in the central basin are unaffected. There is still transport resulting from the upward flux of bedrock groundwater entering the regolith and subsequently the water column and there is still mixing. With the loss of the standing water compartment in the outer basin, however, there are some significant changes to conditions in the regolith compartments.

Firstly, with the loss of the water compartment – at $t = t_{aqu}^{Outer}$, all the inventory in the water compartment must be accounted for. In practice the model contains numerous switches based on the timing parameters in Section 5.1.2. For example, since by definition, $F_{wat,bto}^{Outer} = F_{upp,tpi}^{Outer} = 0$, it is possible to set

$$\lambda_{wat,upp}^{Outer} = \begin{cases} 0 & t \le t_{aqu}^{Outer} \\ 10^9 & t > t_{aqu}^{Outer} \end{cases}, \tag{6}$$

this has two functions, i) to transfer any residual activity at the end of the aquatic period to the top soil and ii) to maintain it as zero thereafter. The shrinking water column therefore drains through the upper regolith and, because the inventory is then effectively zero and because the compartment is disconnected from other compartments in the network, the inventory remains zero. This complements the loss from the water compartment to lateral compartments. This procedure is used for all "lost" compartments when they are no longer active.

The second major change is that the regolith compartments are no longer covered by water and the net precipitation must be accounted for. With the compartment structure of the GEMA-Site modules, vertical and lateral flux balance is to be considered. At the upper regolith of the outer basin, the top boundary receives net infiltration, the balance between fluxes at the top face of the upper regolith compartment:

$$F_{upp,tpi}^{Outer} = PA_{obj}, \quad F_{upp,tpo}^{Outer} = EA_{obj} \tag{7}$$

As this input moves through the compartment the altered hydrology in the basin means that there is movement vertically down through the compartment as well as laterally out of the compartment. Because of the boundary conditions (the surface of the Outer module is the most elevated part of the basin) there are no inputs or outputs at the upstream boundaries and is no input from the downstream boundary.

$$F^{Outer}_{upp,upi} = F^{Outer}_{upp,upo} = 0, \qquad F^{Outer}_{upp,dni} = 0 \tag{8}$$

There is no upward movement in the regolith column at this stage, defining

$$F^{Outer}_{upp,bti} = 0 \tag{9}$$

Only the downstream flux and the vertical infiltration terms remain to be addressed. From balance the volumetric flux concerned is $(P-E)A_{obj}$ m^3 year^{-1}. These are partitioned according to

$$\begin{aligned} F^{Outer}_{upp,dno} &= \phi^{Outer}_{upp}\,(P-E)\,A_{obj} \\ F^{Outer}_{upp,bto} &= \left(1-\phi^{Outer}_{upp}\right)(P-E)\,A_{obj} \end{aligned} \tag{10}$$

The parameter ϕ^{Outer}_{upp} therefore characterises the flow system in the outer basin. It has a counterparts in the mid- and lower regolith compartments that describe the flow vectors in the outer basin.

Numerically the values for these two model parameters must be based on results from the regional groundwater model using MIKE-SHE (Bosson *et al*., 2010). Appendix 2 shows how the numerical values are related to the Bosson *et al*. "average object". The ϕ^{Outer}_{i} are derived as

$$\phi^{Outer}_{i} = \frac{F_{subCatch,i}}{\sum_{i=Low,Mid,Upp} F_{subCatch,i}} \tag{11}$$

where $F_{subCatch,i}$, m^3 year^{-1}, are the fluxes out of what Avila *et al*. identify as the sub-catchment area of the "average object". The flux map for the "average object is discussed in Appendix 2. From this

$$\begin{aligned} \phi^{Outer}_{Upp} &= 0.697 \\ \phi^{Outer}_{Mid} &= 0.282 \\ \phi^{Outer}_{Low} &= 1-\phi^{Outer}_{Upp}-\phi^{Outer}_{Mid} = 0.021 \end{aligned} \quad . \tag{12}$$

Clearly these are important parameters and this initial model provides scope for further investigation.

Equations (7) to (11) define the water balance in the upper regolith of the outer basin. They also feed into the mid-and lower regolith layers. As there are no other inputs to the outer basin, mass balance in the mid-regolith has

$$F^{Outer}_{mid,tpi} = F^{Outer}_{upp,bto} = \phi^{Outer}_{upp}\,(P-E)\,A_{obj}\,, \tag{13}$$

so that fluxes in the compartments of the module are related directly to the inputs shown in Table 1. In the case of water fluxes the P, E and v_{geo}. This simplifies the task of maintaining mass balance. The coding of the model therefore uses

$$
\begin{aligned}
F^{Outer}_{mid,tpi} &= F^{Outer}_{upp,bto} \\
F^{Outer}_{mid,bto} &= F^{Outer}_{mid,tpi} - F^{Outer}_{mid,dno} \\
F^{Outer}_{mid,dno} &= \phi^{Outer}_{upp}\left(F^{Outer}_{upp,tpi} - F^{Outer}_{upp,tpo}\right) \\
F^{Outer}_{mid,tpo} &= F^{Outer}_{mid,bti} = F^{Outer}_{mid,dni} = F^{Outer}_{mid,upi} = F^{Outer}_{mid,upo} = 0
\end{aligned}
\tag{14}
$$

Similarly for the lower regolith compartment,

$$
\begin{aligned}
F^{Outer}_{low,tpi} &= F^{Outer}_{mid,bto} \\
F^{Outer}_{low,bto} &= F^{Outer}_{low,tpi} \\
F^{Outer}_{low,bti} &= F^{Outer}_{low,tpo} = F^{Outer}_{low,bto} = F^{Outer}_{low,dni} = F^{Outer}_{low,upi} = F^{Outer}_{low,upo} = 0
\end{aligned}
\tag{15}
$$

The flows in the regolith of the outer basin are therefore driven by the balance between precipitation and evapotranspiration.

The Outer basin collects water that must then flow through the rest of the basin. During the evolution this process – the change to the direction and magnitude of the flow vectors – is repeated, first for the Inner basin and then for the Central basin. The derivation of the water fluxes proceeds in a similar manner. As can be seen, the full development of the expressions is rather detailed. Appendix 2 provides the detail.

5.1.4. Evolution of compartment properties

In addition to the changes in the flow system the most obvious impact on the state of the system during the evolution are the changes to the compartments themselves. Water disappears from the basin and sediment is deposited, plants grow and decay. Some of these changes are noted in the preceding section in relation to the difference between mass fluxes for sedimentation and resuspension/erosion.

The compartment thickness change as a combination of two processes – landrise and net sedimentation. This is interpreted to mean that the lower and mid-regolith compartments are constant in thickness. Sedimentation affects the upper regolith and also reduces the water depth. Additionally, the transition from wetland sediments to agricultural soil is also accompanied by some compaction and changes in associated parameters. Transfers of activity are handled as sudden transitions in a similar way to the conservation rule in Equation (6) for the loss of the water cover in each module.

In general, the compartment thickness is given by

$$
l(t) = l_0 + \int_0^t \dot{l} dt \tag{16}
$$

where the change in thickness is a combination of sedimentation and uplift, as appropriate to the compartment. For the upper regolith therefore

$$l(t) = \begin{cases} l_{agri} & t \geq t_{agri} \\ l_0 + \dfrac{\left(s_{ned} - s_{upp}\right)}{\rho_{bulk}(t)} t_{sea} + \dfrac{m_{nat}\kappa_{nat}}{f_{pC}\rho_{bulk}(t)}\left(t - t_{sea}\right) & t_{sea} \leq t < t_{agri} \\ l_0 + \dfrac{\left(s_{ned} - s_{upp}\right)}{\rho_{bulk}(t)} t & t < t_{sea} \end{cases} . \quad (17)$$

After conversion to agricultural conditions the soil is assumed to be constant thickness but prior to that there is accumulation in the sea stage (balance of deposition and resuspension in the basin) and the lake and wetland stages by deposition of decaying plant material, with effective net deposition rate

$$\dot{l}_{upper} = \frac{m_{nat}\kappa_{nat}}{f_{pC}\rho_{bulk}(t)} . \quad (18)$$

with the m_{nat} = 6 kgC m^{-2} is the biomass of primary producers and κ_{nat} year^{-1} is fractional the growth rate of primary producers (data from Avila *et al*., 2010). Conversion to dry weight uses the fractional mass of carbon per unit dry weight, f_{pC} = 0.444 kgC kg^{-1} dw, based on the stoichiometry of starch, $C_6O_5H_{10}$. The density of the material changes in time, according to the type of material (see below). Note that the same net accumulation of organic material is assumed in both the lake and wetland stages[3].

For the water column, therefore

$$l(t) = \begin{cases} l_{min} & t \geq t_{aqu} \\ l_0 + \dot{l}_{uplift} t_{sea} + \left(\dot{l}_{uplift} - \dot{l}_{upper}\right)\left(t - t_{sea}\right) & t_{sea} \leq t < t_{aqu} \\ l_0 + \dot{l}_{uplift} t & t < t_{sea} \end{cases} \quad (19)$$

The GEMA-Site model is configured to allow most parameters to evolve in a similar way to the compartment thickness in Equation (17). In order to make most efficient use of the Avila *et al*. database, however, switches were also used for parameters such as k_ds, densities, porosities and volumetric moisture content. These were related to specific measurements in the SR-Site database, here illustrated by the example of porosity of the upper regolith:

$$\varepsilon_{upp} = \begin{cases} \varepsilon_{peat} & t \geq t_{aqu} \\ \varepsilon_{glacialClay} & t < t_{aqu} \end{cases} . \quad (20)$$

This first approximation leads to step changes in properties and may be reconsidered for future model developments if required.

[3] These mass fluxes are not part of the formal mass-balance scheme of the dynamic compartments. The carbon comes predominantly from the atmosphere (> 95%) via the vegetation, neither of which are dynamic compartments in the model.

5.1.5. Radionuclides and releases

For the example application of the model reported here key radionuclides from the SR-Site licence applications and others of lower consequence but interesting features are considered:

- ^{79}Se – as a low k_d fission product with potentially high uptake in vegetation
- ^{129}I – radionuclide with the highest LDF (landscape dose factor) reported by Avila *et al*. (2010); fission product with low but redox sensitive k_d,
- ^{94}Nb – relatively strongly sorbing fission product with major contribution to dose from γ-irradiation, and
- The ^{226}Ra and daughters (explicitly ^{210}Pb and ^{210}Po) – decay chain with moderate to strong sorption and a range of half-lives; the α-emitter with the highest LDF in SR-Site.

Radionuclide specific data for the GEMA-Site application are given in Appendix 3.

To illustrate the response of the model, release from the bedrock *to the lowest part* of the basin is assumed. This is consistent with the information in Lindborg (2010). Therefore, in the three module representation of the basin, only the *Central basin* receives radionuclide input (as illustrated in Figure 8) and, similarly, the only input of groundwater from the implied fracture is to this lower module.

1 Bq year^{-1} of each of ^{79}Se, ^{94}Nb, ^{129}I and ^{226}Ra is released throughout the duration of the simulation. ^{210}Pb and ^{210}Po grow in and short lived daughters in the decay chain (including ^{222}Rn) are included by adding the dose per unit exposure values to those of their explicitly modelled parent.

5.2. Results for system evolution

5.2.1. Physical model

The timing events calculated by the model are shown in Table 5, for the dataset described above. In this model only the Central basin is converted to agriculture and this takes place at 19000 year after the start of the release. Note the relatively short duration of the lake/bay phase of the three modules following emergence from the sea. This is affected by uplift and accumulation of organic material. The lakes' persistence is around 800 years for the Outer and Inner basins and 650 years for the Inner basin. The short existence of the lakes suggests that the use of the hydrology during the lake period as representative of the evolving basin is questionable.

Figure 10 shows how the depth of water and the thickness of the regolith layers in the three modules change according to the rules and timings. The assumed 5 m difference in the topographic heights of the three modules produces a different response from the three areas. Though barely discernible in Figure 10(a), there is a small change in the gradient of the rate of change of water depth that coincides with the start of net sedimentation in each of the basins during the aquatic phase. As shown in Figure 10(b), coincident with this is the increasing thickness of the upper regolith caused principally by the formation of a peat layer resulting from decaying vegetation. This increases until the end of the simulation at 20 kyear for the non-cultivated Outer and Inner basins. On transition to agriculture in the Central basin however, the drained peat is assumed to be compacted to a thickness suitable for agricultural purposes. This is maintained until the end of the simulation.

Table 5: Events in the evolution of the model basin. Times of transition are given by Equation (2) and the data in Table 3. The influence these have on compartment thickness in the modules in shown in Figure 10.

Time of event [year]	Outer basin	Inner basin	Central basin
End of sea period, t_{sea}	10833	11482	12500
End of lake period, t_{aqu}	11666	12315	13148
Lake persistence	833	833	648
Transition to agriculture, t_{agri}	No conversion	No conversion	19000

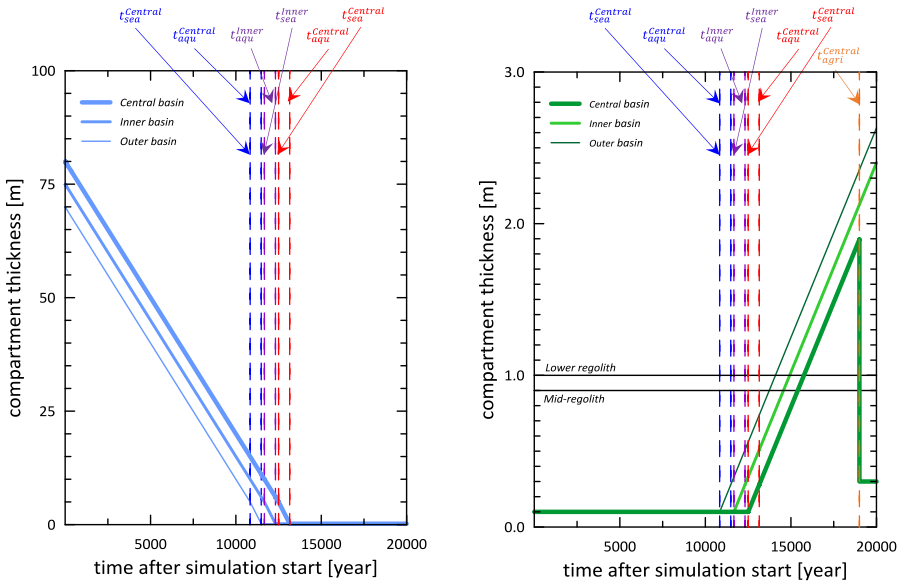

(a) water depth (b) regolith compartment thickness

Figure 10: Evolution of compartment thickness. While lower and mid-regolith in all three modules of the basin are assumed constant the water and upper regolith thicknesses vary in time as described by Section 5.1.4. Timing of the transitions is indicated. Until the end of the sea stage there is zero net sedimentation. Thereafter deposition of peat is included and the rate of reduction of the water column changes from the pure uplift rate (cf. Equation (19)).

5.2.2. Narrative for radionuclide transport and accumulation

Figure 11 illustrates the fate of radionuclides released into the lower regolith of the Central basin. The weakly sorbing ^{129}I and highly sorbing ^{226}Ra are used to illustrate key features of the model. Inventories for each of the compartments in the modules are shown. There is a wide dynamic range, for the 2×10^4 Bq of each radionuclides released over the period of the simulation.

For ^{129}I most of the released activity is lost from the system at the end of the simulation (the *sink* curve), whereas for ^{226}Ra most of the activity is retained in the lower regolith of the Central basin. There is some redistribution of the ^{129}I to the Inner and Outer basins. For ^{226}Ra the inventory in each of the compartments of these two basins is less than 10^{-6} Bq and so is not shown.

Key to understanding the dynamics of radionuclide transport and accumulation in the basin is the evolution of the flow system as modelled. The top plot in Figure 11, shows the evolution of the water fluxes *out* of the compartments in the Central basin. These change in response to the changes in the Inner and Central basin hydrology. Agricultural doses are only derived from the Central basin in this model so only this is the focus of attention in this narrative of the inner basin.

Release to the lower regolith of the Central basin starts at year zero. The upwards flux driving this originates as a result of the regional topography. Compared to the water fluxes in the water column of the sea stages the flow is small but nevertheless it causes a steady increase in the inventory of both ^{129}I and ^{226}Ra in the regolith layers. The water inventories of ^{129}I in the sea water of the three modules in the basin show close to a factor of ten between each, reflecting the depths of the three modules and the fact that the areas of the three modules are in a ratio of 100 to 10 to 1. This means that water column concentrations are similar in each module.

The Outer basin first emerges from the sea at year 10833. By the final emergence of the Outer basin at 11666, there is a change to the flow system. While there is a constant head above the Outer basin, the porewater is relatively immobile. When the head changes, with net infiltration at the upper surface of the upper regolith, the porewater begins to move. Water captured in the Outer basin is directed to the Inner basin and the inventory of the water at the end of the aquatic phase is directed down into the upper regolith and out downstream. This affects the inventory in the Inner basin but, so far, has no effect on the Central basin inventories because the water entering the Inner basin is directed upwards to the water column of the Inner basin, with no down gradient flow to the Central basin. The effect of these changes can be seen in the inventories of ^{129}I in the Inner basin.

Evolution of inventories in the Central basin is relatively unperturbed by the changes in the Outer basin. However, in the period between 11666 and 13148 (end of Central basin aquatic period) there is a clear effect on the inventories in all parts of the basin. A key change takes place at the end of the aquatic period of the Inner basin where there is no longer a discharge vertically upwards to the water column. At this time (year 12315) the captured net precipitation in the Outer and Inner basins is directed into the Central basin. This has two effects depending on the k_d of the radionuclide concerned.

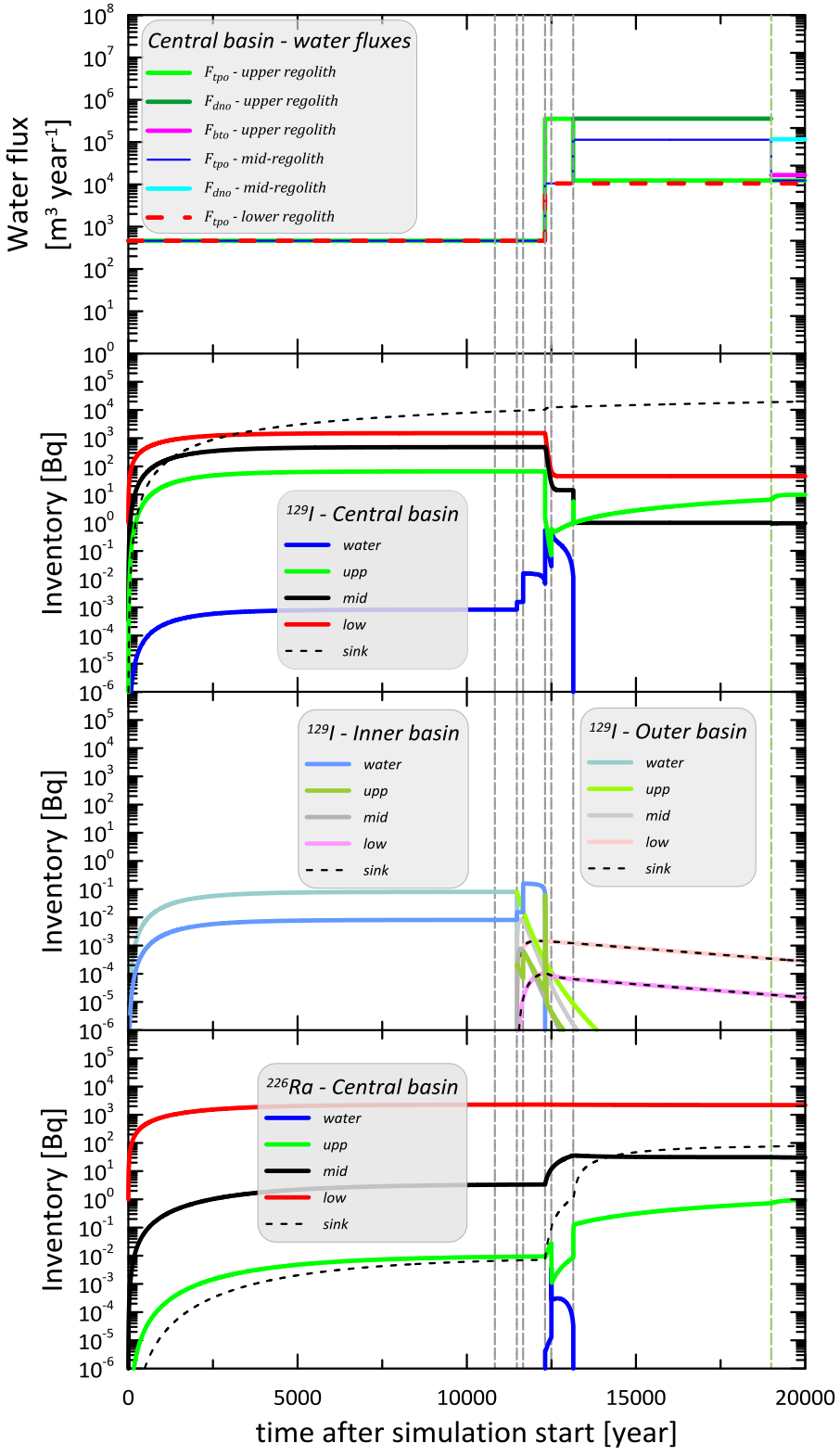

Figure 11. Evolution of radionuclide inventories in response to changes in hydrology. Results for ^{129}I in the Central and Outer and Inner basins and ^{226}Ra in the Central basin are shown. The changes in water fluxes through the Central basin (in response to changes in the Outer and Inner basins) are also shown in relation to the timing of changes.

The high k_d of ^{226}Ra means that accumulation in the lower regolith continues, with the inventory in dynamic equilibrium, even beyond the transition. Nevertheless, the increase in flux through the top of the lower regolith (changing from 10^3 to 3.36×10^4 m^3 $year^{-1}$) mobilises more of the stored inventory leading to a rise in the inventories of the mid- and upper regolith.

By the time of the filling of the remaining lake in the Central basin at year 13148 the ^{226}Ra inventory in the mid-regolith is in equilibrium but the upper regolith inventory continues to increase as a result of the net upward flow. At the time of transition to agriculture at year 19000 the inventory in the upper regolith is over two orders of magnitude higher than the equilibrium value with no evolution. The change in the flow system also increases the amount of ^{226}Ra that is lost downstream. The majority of the release remains in the lower regolith, however.

For the low k_d ^{129}I the increased flow through the Central basin has the opposite effect on the inventory of the upper regolith. The effect of the remobilisation seen for ^{226}Ra is again apparent in that the inventory of the lower and mid-regolith layers are immediately diminished as a result of the more than thirty times increase in flux through the lower regolith as well as the increased inflow via the mid-regolith (485 times higher than the initial water flux through the Central-basin's mid-regolith). The result of this increased throughput is to wash-out the accumulated material in the upper regolith. With the final transformation to wetland in the Central basin at year 13148 the lower and mid-regolith layers again reach dynamic equilibrium and the through flow leads to a gradual increase in the content of the upper regolith, albeit at a lower level than the accumulation at earlier times. The sharp drop in dose from ^{79}Se and ^{129}I at the start of the wetland period corresponds to the assumed time taken for the terrestrial ecosystem to become established. During this *colonisation period* there is a lack of vegetation for consumption by animals or humans.

At the time of transition to agriculture – by human action to change the drainage system – at year 19000 in this simulation, the inventory of ^{129}I is around an order of magnitude lower than the highest accumulation whereas the ^{226}Ra inventory is around an order of magnitude higher.

The change to an agricultural system has another impact on the upper regolith content. At this stage of the evolution there is exchange with the mid-regolith via infiltration and evapotranspiration. The main input to the mid-regolith comes from the circulation through the lower regolith from the Outer and Inner basins. Outflow from the agricultural land is via emplaced drainage in the mid-regolith layer (as shown in the top plot of Figure 11). After the emplacement of drains there is a mixing of water in the upper regolith. There is net infiltration to the mid-regolith but this is part of an overall re-circulation between mid- and upper regolith. There is a net increase in the content of the upper regolith. This may seem contradictory. The reason is that drainage during the wetland period is via the upper regolith whereas in the agricultural system it is via the emplaced drains in the mid-regolith.

The impact on the assessment of dose arising from this bifurcated response of the radionuclides in the hydrologic system on the results of the dose assessment are discussed in the next chapter.

6. Dose assessment and sensitivity study

6.1. Overview of calculational cases

The model description in Sections 4 and 5 above is formulated around the characteristics of Basin 116 (see Figure 5 and 6) currently beneath the surface if the Öregrundsgrepen. There are many similar basins in the present-day terrestrial landscape to the southwest of the repository location and there will be many more in the emerging landscape to the northeast over the coming millennia.

The hydrogeology of the other basins in the landscape will be sufficiently similar to that in the reference basin for the description of their evolving groundwater vectors and the changes they undergo to be employed in models of other basins. What will differ will be the data descriptions. This is a major modelling assumption underlying GEMA-Site usage.

The factors that differentiate the basins are largely, therefore, matters of *geometry*: the overall basin area, the relative sizes of the Outer, Inner and Central basins, the thicknesses of the regolith layers, the topographic minima and maxima and the initial depth of water, etc. For illustrative purposes, the variability in dose response to different module areas is addressed here.

The reference model uses ratios of $10^7 : 10^6 : 10^5$ m^2 for the Outer, Inner and Central basins respectively. This defines the 7-6-5 geometry of the basin as the reference case here. Review of the basin data from Lindborg (2010) in Table 2 suggests a range of options for variant geometries. The reference basin is already towards the higher end of the ensemble. For comparison therefore a small basin is considered with 5-4-4 geometry ($10^5 : 10^4 : 10^4$ m^2, Outer, Inner, Central areas respectively). Other variants are listed in Table 6.

The purpose of the biosphere model is not only to describe the *transport* of radionuclides in the biosphere, it also accounts for *accumulation* in near surface media. The reference model allows time for accumulation, particularly of the highly sorbing radionuclides, ^{94}Nb and the members of the ^{226}Ra chain. Imposition of agriculture at 19 kyear is therefore the reference case. The earliest transition would be at the end of the lake period, coincident with the silting up of the lake at $t = t_{aqu}^{Central}$. Doses from this scenario are compared with the reference as well as with transition at 19.95 kyear (allowing for agriculture to be practiced for 50 years before the end of the simulation. An intermediate time (15.5 kyear) is also evaluated.

In SR-site drinking water is assumed to be sourced from a bedrock well. This lies outside the scope of the biosphere model and integrating such a scenario with the unit release to the biosphere on which the LDFs are based is fraught with inconsistency; is the well concentration based on the same 1 Bq per year as is released to the base of the lower regolith? Is the *average* well dilution cited by Lindborg (2010) appropriate? It is not clear that these features are interpreted in a conservative manner in SR-site.

Doses in GEMA-Site can be calculated assuming a variety of sources of drinking water. When a lake exists it is assumed that this is the source. During the wetland period there would be some standing water at different times during the year but this

Table 6. Variant cases used in the deterministic sensitivity analysis. The reference case is defined as the 7-6-5 basin, transition to agriculture at 19 kyear with the drainage system used for water supplies, no irrigation.

		module area, m^2		
Basin geometry	**id**	A_{Outer}	A_{Inner}	$A_{Central}$
Large basin	7-6-6	1.0E+07	1.0E+06	1.0E+06
Reference	**7-6-5**	**1.0E+07**	**1.0E+06**	**1.0E+05**
Small agri.	7-6-4	1.0E+07	1.0E+06	1.0E+04
Equal modules	5-5-5	1.0E+05	1.0E+05	1.0E+05
Small basin, small agri.	5-4-4	1.0E+05	1.0E+04	1.0E+04

Time of transition to agriculture	t_{agri} **kyear**
As soon as possible	13.148
alternative	15.5
Reference	**19**
As late as possible	19.95
Never agriculture	> 20

Water resource	
Reference	**drainage system**
Alternatives	shallow well
	shallow well, irrig.
	no local water

is not assumed to be consumed by the human population. Agriculture necessitates an emplaced drainage system to divert the captured net infiltration in the whole basin away from the agricultural upper regolith. This is one potential source of domestic and agricultural water. Although the water column of the drainage system is not explicitly modelled the concentration of water is defined by the radionuclide flux into the drainage system and the total flow in the drainage channels:

$$C_{drain} = \begin{cases} \dfrac{\sum_{all\ i} \lambda_{i,dno} N_i}{\sum_{all\ i} F_{i,dno}} & t \geq t_{agri} \\ 0 & t < t_{agri} \end{cases} \text{ Bq m}^{-3}. \quad (20)$$

This arises from Figure 9e so that the active loss fluxes are $F_{dno}^{Inner.Upp}$ and $F_{dno}^{Central.mid}$.

Alternatively a shallow well abstracting water from the lower regolith can be assumed. A final variant assumes that all drinking water is obtained from sources external to the model, ie, uncontaminated sources. The variants are

$$C_{dw} = \begin{cases} \dfrac{C_{low}}{R_{low}} & t \geq t_{agri}, well\ exists \\ C_{drainage} & t \geq t_{agri}, no\ well \\ C_{wat} & t_{sea} \leq t < t_{aqu} \\ 0 & t < t_{sea} \end{cases} \quad (21)$$

Irrigation is considered to be unlikely given present-day agricultural practices. Nevertheless the most exposed group need not be assumed to comprise commercial producers. The case of a kitchen garden, where home-grown produce is consumed should also be considered. There is little difference between the FEPs leading to accumulation in foodstuffs between this scenario and the standard agricultural scenarios. However, the option to use contaminated water from the drainage system or the shallow well is included. Here results from irrigation of vegetables using five applications of well water are included in the analysis.

6.2. Reference calculation: 7-6-5, 19 kyear, drainage

Results for the dose summed over all pathways for the four radionuclides input to the basin are shown in Figure 12. For ^{226}Ra, the contribution of the long-lived daughters (^{210}Pb and ^{210}Po) are included as these are modelled explicitly in the simulation[4]. Focus is on the dose from the Central basin as this is the only agricultural area assumed in the model. These results illustrate the fundamental workings of the GEMA-Site model.

The influence of k_d is clearly seen. ^{79}Se and ^{129}I are weakly sorbing and for these two there are doses during the sea stage, albeit at low levels, even when allowing for increased concentration as the water levels fall. The doses derived from seawater (fish and crustacea) are similar in each of the modules because the concentrations are the same (see Section 5.2.2). Doses can be differentiated as the water column depth decrease in each module and the upper regolith emerges from the water.

For the more strongly sorbing ^{94}Nb and ^{226}Ra (and ^{210}Pb, ^{210}Po) doses from the Central basin are overwhelmingly dominant. As discussed above, retention in the lower regolith at the release location means that such inventories as do arise in the Inner and Outer basins are insignificant. For the lake period of the Inner basin, there is a small dose from the consumption of natural foodstuffs but this is around four orders of magnitude lower than the corresponding period in the Central basin.

[4] Short-lived decay products from ^{226}Ra, including ^{222}Rn are implicitly included by adding their dose-per-unit-exposure to that of their long-lived parent.

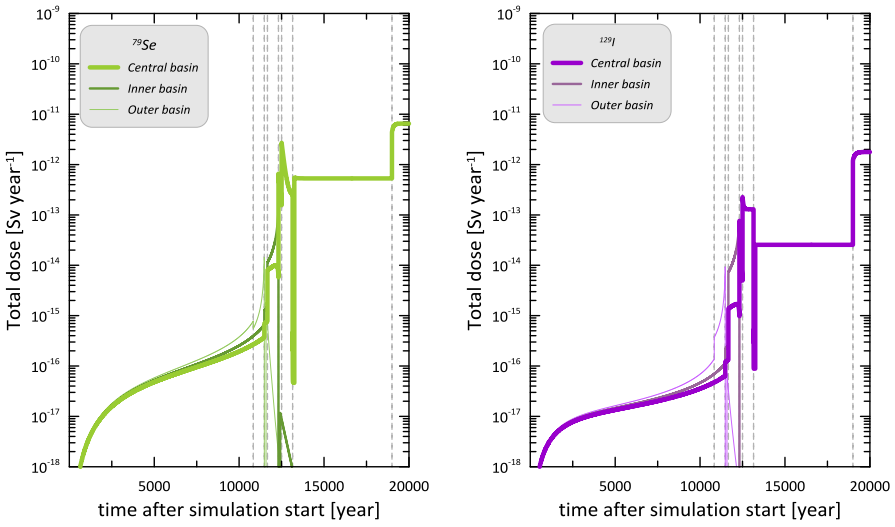

(a) ^{79}Se (b) ^{129}I

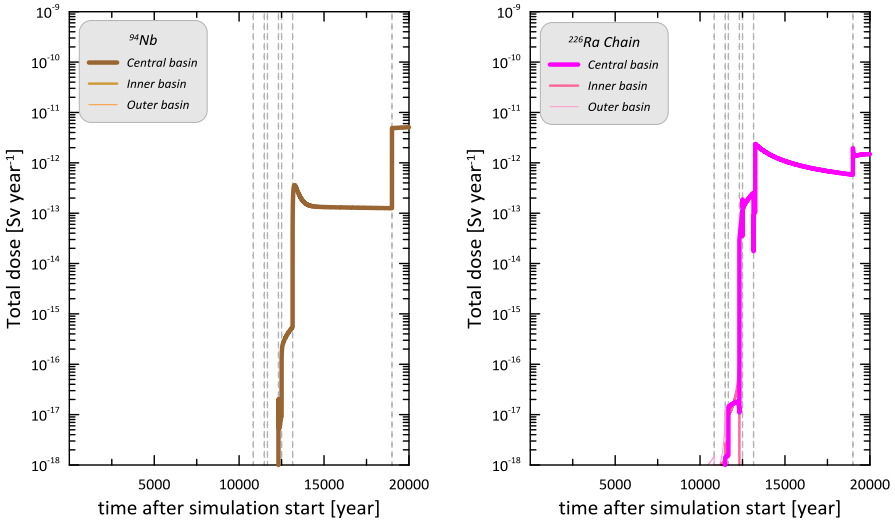

(c) ^{94}Nb (d) ^{226}Ra chain

Figure 12. Dose over all exposure pathways. For each of the radionuclides released the sum over all pathways is plotted for each of the three basins. The dashed lines denote the times of transition for the three modules as set out in Table 5.

Table 7: Results from the GEMA-Site reference model. From the results in Figure 12 the dose just after the transition to agriculture is given, as well as the peak dose over all the simulation and the time of the peak. Doses during the agricultural period in the wetland are given as well as the peak dose in non-agricultural ecosystems. For the peak dose, the three highest exposure pathways are listed. Bold entries denote the highest dose for each of the radionuclides released.

	Dose at t_{agri}		Peak dose	Time of peak	Pathway ranking		
nuclide	**Sv year^{-1}**	**ecosystem**	**Sv year^{-1}**	**year**	**1st**	**2nd**	**3rd**
^{79}Se	**4.4E-12**	**agriculture**	**6.5E-12**	**19355**	**cereal 48%**	***game 20%***	**root veg. 12%**
		lake	2.7E-12	12502	fish 93%	crustacea 6%	drinking water 0.4%
^{94}Nb	**4.9E-12**	**agriculture**	**5.1E-12**	**19814**	**external 95%**	**inhalation 4%**	**cereal 1%**
		wetland	3.6E-13	13255	external 86%	inhalation 14%	berries 0.03%
^{129}I	**1.2E-12**	**agriculture**	**1.8E-12**	**19406**	**cereal 45%**	**milk 18%**	**root veg. 11%**
		lake	2.3E-13	12502	fish 55%	drinking water 29%	crustacea 17%
^{226}Ra chain	2.0E-12	agriculture	2.0E-12	19001	*game 35%*	drinking water 27%	inhalation 18%
		wetland	**2.4E-12**	**13249**	***game 92%***	**inhalation 4%**	**berries 3%**

Doses from the Inner basin over the period of transition from aquatic to terrestrial ecosystems are relatively high in the case of ^{79}Se and ^{129}I. In part this is a consequence of the conservation of activity during the transition as the water column drains through the upper regolith. For ^{129}I there is also a period between the end of the sea period and the end of the aquatic period in the Central basin (year 12500 to year 13148) where there is an apparently high dose. However, this, and other features in the plots for the low k_d nuclides are something of an artefact of the transition and the dataset used. During the aquatic stage of the Central basin the water is assumed to be freshwater with, implicitly, suitable fish species. The spike in the ^{129}I dose is accounted for by the difference in concentration ratio for salt and freshwater fish; that for freshwater is 16 times higher and this accounts for the sudden rise on this transition.

Some of the sharp-edged transitions in the dose vs time plot arise because the current version of the model does not model transitions between ecosystems as a gradual process, rather there are abrupt transitions. The step increase in dose at the time

of the transition to agriculture is more representative of the change in exposure with the advent of agriculture. It is known that agriculture can be practiced in the year following the emplacement of drainage (Biebighauser, 2007) and certainly within five years (Smedema, *et al*., 2004). The potential for the doses on the initial transition is therefore real.

There are transients in some of the dose curves – spikes with decay rates dependent on the characteristics of the radionuclides (for example, the dose from ^{94}Nb and the ^{226}Ra chain after the transition to wetland in year 13148). To account for these SSM's regulatory guidance (SSM, 2008) allows the use of a lifetime averaged annual dose to account for transients in the dose and Avila *et al*. (2010) therefore use the 50-year average:

$$\left\langle D_{50}\left(t\right)\right\rangle = \frac{1}{50}\int_{t}^{t+50} D_{tot}\left(t'\right)dt' \,. \tag{22}$$

The dominance of the agricultural ecosystem is illustrated in Table 7. In the discussion here a range of dose is presented: the peak dose and the dose just after transition to farmland. This ranges encompasses the transients without the need to evaluate $\left\langle D_{50}\left(t\right)\right\rangle$ directly. Because the ^{226}Ra chain dose peaks on the transition to wetland, Table 7 shows the peak dose during the agricultural period as well as the peak during all other stages of ecosystem development. The pathways contributing to dose during these periods express the characteristics of the different radionuclides.

During the agricultural phase the more mobile radionuclides have highest doses from cereal consumption – both ^{79}Se and ^{129}I have high soil-plant concentration ratios. Similarly root vegetable consumption is important, as well as milk consumption for ^{129}I. Somewhat surprisingly game is flagged for ^{79}Se during the agricultural phase and game consumption is the dominant pathway for the ^{226}Ra chain in both the agricultural and non-agricultural ecosystems (see below). During the lake phase the high uptake in freshwater fish for ^{79}Se and ^{129}I gives a high dose coinciding with the reduced water exchange in the water column of the Central basin's lake at this time. There is a slow decrease in the overall activity in the lake system.

For ^{94}Nb, a strong γ-emitter external and inhalation doses dominate. During the agricultural period there is a contribution from cereal consumption and berries during the wetland phase. The dynamics of the wetland dose reflect the changes to the hydrology of the basin during the evolution. With the loss of the water column the net upward flux of radionuclides into the lake, and subsequent flushing from the system stops. Drainage still takes place but now it is through the wetland where retention of the highly sorbing ^{94}Nb can take place. Prior to the wetland forming there had also been accumulation in the upper regolith – as lake bed sediment – but activity concentrations there were shielded by the water column. Drainage through the upper regolith of the wetland gradually decreases the concentration in this upper regolith layer. Doses gradually fall from a peak close to the start of the wetland phase.

The situation with ^{226}Ra is complicated by the way in which the dose from game consumption is modelled. As noted in Chapter 2, the formulation here is directly adopted from that in SR-Site (See Appendix 2).

Analysis of the contributions to dose from the ^{226}Ra decay chain shows that ^{210}Po dominates and that the dose from game consumption is by far the highest component during the wetland phase. The reasons for this are twofold:

1. the exposure pathway model employed by SKB in SR-Site,
2. the interpretation of surface hydrology in GEMA-Site.

Dose from game is given (in Appendix 1 here) as

$$D_{game} = H_{ing} f_{game} I_{game} Z_{game} C_{game} \quad (23)$$

with

$$C_{game} = CR_{game} Z_{berries} CR_{natural} C_{topSoil} \quad (24)$$

Equation (23) gives the dose from ingestion of game muscle (allowing for the fraction of contaminated game in the diet) including the concentration in game. Equation (24) relates the concentration in game to the assumed foodstuff consumed by the game animals, ie, berries. There are conversion factors to convert from dry weight of berries to the consumed fresh weight and for the muscle content of the carcass.

Equation (24) contains two concentration ratios: berry relative to soil, $CR_{natural}$ (Bq kg^{-1} dw berry)(Bq kg^{-1} dw soil)$^{-1}$ and game relative to berry, CR_{game} (Bq kg^{-1} dw) (Bq kg^{-1} dw berry). Appendix 3 lists the data values used in the calculations here.[5] The tables summarising nuclide specific data in Appendix 3 show that there are particularly high game CRs for ^{79}Se, ^{210}Po and, to a lesser degree ^{129}I, as well as a high natural foodstuff CR ^{79}Se. The natural foodstuff CR for both ^{129}I and ^{210}Po are also relatively high. Together, therefore, these factors combine to elevate the game dose contribution to the total pathway dose.

It is the *transport and accumulation* processes in GEMA-Site that are required to boost the ^{210}Po dose to prominence. While ^{79}Se and ^{129}I are concentrated in berries and then game, their concentration in the top soil of the wetland is relatively low – they are weakly sorbing and so do not accumulate significantly at any stage of the evolution. This cannot be said of ^{210}Po which is retained in the upper regolith. During the lake phase there is appreciable accumulation of sorbed and ingrowing ^{210}Po during the lake stage of the central basin. This accumulation combined with the high uptake in berries and then game, *as modelled*, accounts for prominence of game in the dose from ^{210}Po and thereby the ^{226}Ra chain.

The significance of this can be questioned, however. The model for game dose expressed in Equations (23) and (24) is somewhat simplistic – certainly less sophisticated than the treatment of accumulations in domesticated animals in the agricultural ecosystem model. It is only when this simplistic model is combined with the detail of the GEMA-site evolving hydrology model that the game dose becomes noticeable. This result highlights the need to represent the exposure pathways for non-agricultural ecosystems in a more consistent manner. Nevertheless the functionality of the evolving hydrology in GEMA-Site is amply demonstrated.

GEMA-Site's *raison d'être* is the investigation of the influence of those FEPs involved in system evolution on calculated dose. In the following sections the GEMA-site model's response to variants of the Reference Model are discussed in order to better illustrate these aspects of the model. Results for the peak dose over all time in the reference model are used to normalise the peak dose from the simulation and the dose just after the transition to agriculture. This gives the range of results as plotted.

[5] The concentration ratios used in GEMA-Site take the traditional approach in that they are defined with respect to the dry mass of the foodstuff. The values used here are converted from data in Nordén *et al*. (2010) which uses Bq kg^{-1} carbon content.

6.3. Time of transition to agriculture

Figure 13 compares results of the reference case dose evolution with the alternative where transition of the Central basin is carried out as soon as possible at the end of the lake phase. Figure 14 plots the range of results for five variants on the time of transition to agriculture.

The issue here is the extent to which longer term accumulations in the regolith can give rise to higher doses in agricultural systems. Comparing results from the reference basin using surface water resources and transition at 19 kyear with the "as soon as possible" variant, with $t_{agri} = t_{aqu}$ = 13148 CE shows that the long-term doses are similar in each case. The small short transient around 19 kyear for the ^{226}Ra chain is also close to the steady-state result. Results for ^{94}Nb highlight the mechanisms. The flow system in the agricultural land (see Figure 9e) acts to transfer activity to the upper regolith – the distribution of activity in the regolith at time of transition does not give the highest concentration in agricultural soil, there is still some redistribution.

This contrasts with the SR-Site model of agricultural land where only washout is represented. Consequently the dose in the year following conversion to farmland is always highest and it decreases in time. SKB use the 50-year averaged dose to calculate the LDF to account for this transient. Overall the effect is small – much less than a factor of two in the GEMA-Site reference basin.

With the transition to agricultural land as-soon-as-possible the evolution shows a similar sudden increase following the start of agriculture. Each of ^{129}I and the ^{226}Ra chain show a slow increase upto the equilibrium values. This takes on the order of 500 years. For ^{94}Nb (with relatively high k_ds in each of the three regolith layers) the time to equilibrium is significantly longer, more than 7 kyear. ^{79}Se shows equilibrium almost instantaneously – in the first few hundred years post transition there is an insignificantly higher maximum.

These dynamics are of interest. Jansson *et al*. (2006) have reviewed the historical records of rural Sweden over the last four hundred years for the Misterhult parish on the south-east coast. There have been significant changes in land use and ownership in this time. Nevertheless some agricultural areas have remained in use for several hundred years but this is relatively uncommon. Doses over a few hundred years post-transition might give a reasonable expression of the radiological impact but longer time periods are correspondingly uncertain.

These results suggest that the timing of the transition has little impact. The maximum dose is similar in each case. Only the "never agricultural land" results are lower, emphasising the significance of agricultural ecosystems in dose assessment. The exception is the dose for the ^{226}Ra chain, as discussed, where the natural ecosystem dominates. A different response for strongly and weakly sorbing nuclides is also noticeable. For ^{79}Se and ^{129}I the highest results occur at earlier times whereas for ^{94}Nb and the ^{226}Ra chain the highest consequences arise for longer accumulation.

Because the dose immediately after transition is an important indicator of dose from agricultural systems, the lower bound is of interest and the role of accumulation is apparent. For ^{79}Se there is significant prior accumulation in the lake bed and, while this is rapidly washed out with the altered regolith flow system during the wetland phase, there is a tendency for *re*-accumulation in wetland upper regolith. This is seen in the increase of the minima of the plots in Figure 14 with increasing t_{agri}. This accumulating trend is seen for the other three radionuclides in the release.

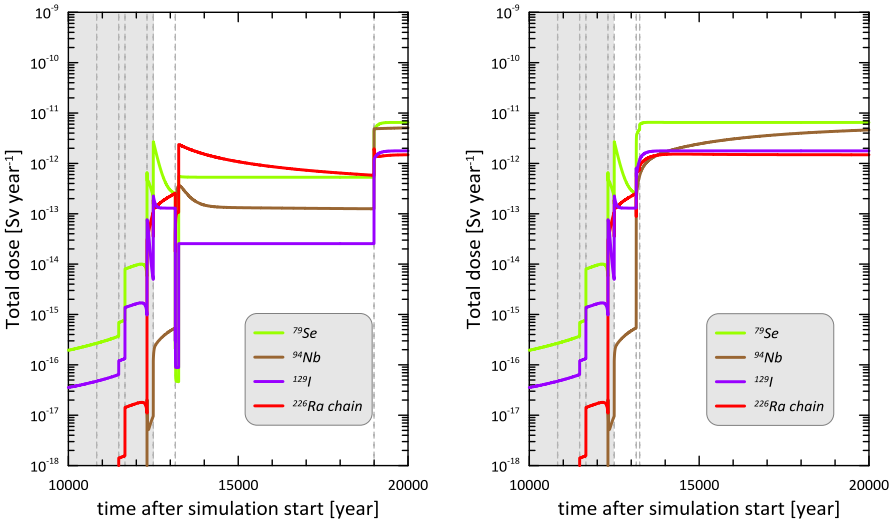

(a) reference case (t_{agri} = 19 kyear)

(b) t_{agri} = 13.148 kyear, "as soon as possible", after the end of the lake stage of the Central basin

Figure 13: Evolution of doses using the reference basin model – influence of time of transition to agriculture (t_{agri}) on dose. Default case with transition to agriculture at 19 kyear compared to the case with transition "as soon as possible" (at the end of the lake stage of the Central basin). Dashed lines indicate transitions to the flow system, shaded area denotes transitions for Outer and Inner basin ecosystems.

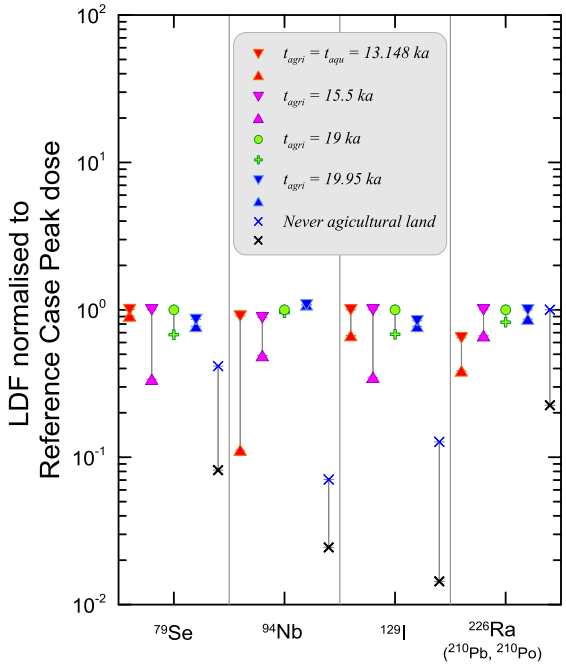

Figure 14: Deterministic sensitivity results for different times of transition to agriculture in using the 7-6-5 reference case basin model. Results normalised to reference case.

Overall the lack of sensitivity to time of transition to agriculture in these results is a consequence of the model. The 19 kyear transition is a useful indicator of what the "landscape dose factor" should be. SKB's approach, which estimated doses from agricultural systems at all times when land surface was available, with the LDF being taken as the maximum of this set of doses, produces a reasonable estimate of the potential radiological impact.

6.4. Basin geometry

Figure 15 illustrates the differences in the evolution of dose caused by alternate basin geometries. The 7-6-5 reference case has areas in the ratio 10^7:10^6:10^5 m^2 for the outer, inner and central basins, respectively. The variants shown here are the 5-5-5 case, a relatively small total basin with the same agricultural area as the reference; the second variant is a smaller basin with the inner and central basins each 10^4 m^2 (the 5-4-4 geometry). In this variation the time of transition to agriculture is maintained at 19 kyear.

The areas of the basins differ: the collecting area for net infiltration therefore gives significantly different groundwater flow vectors in the basin. These variants lead to systems with significantly different hydrological characteristics. Doses during the transition from marine to terrestrial ecosystems vary considerably and doses at times before the formation of the lake in the central basins are notably different in each case. This makes a discussion of the details somewhat involved.

Releases to basins with different sizes show differences not only in magnitude of dose but also in terms of dynamics. The ^{226}Ra chain in Figure 15 illustrates this. Changes to the ecosystem of the central basin on isolation of the lake (at the transition denoted by the grey shaded area) lead to relatively high concentration in lake water. In the 5-5-5 case this decreases slowly whereas the decay is much more rapid in the 5-4-4 case. Similarly, post the agriculture transition, the rate of increase of dose towards the equilibrium value is different for the two alternative flow system representations. These features are a result of the differences in the regolith groundwater flow field embodied in the definition of the model. The dynamics of the ^{79}Se dose also provide instructive examples on the influence of the flow system model.

In these two smaller basin models (compared to the reference 7-6-5 geometry) the ecosystem with the maximum dose also shows some variation. In the 7-6-5 case the wetland ecosystem has the highest ^{226}Ra chain dose in the period after its formation. In each of the 5-5-5 and 5-4-4 cases the agricultural ecosystem dominates, suggesting the importance of the natural ecosystem in the reference case may be overstated.

Figure 16 shows the range of values for five variant area models:

- small basin, with small agricultural area (5-5-5 geometry), small overall basin
- equal modules (5-5-5 geometry), small overall basin
- small agriculture (7-6-4 geometry), similar to the reference case with a smaller central area
- Reference case (7-6-5 geometry)
- Large basin (7-6-6 geometry), a simple case with a central area ten times larger than the reference.

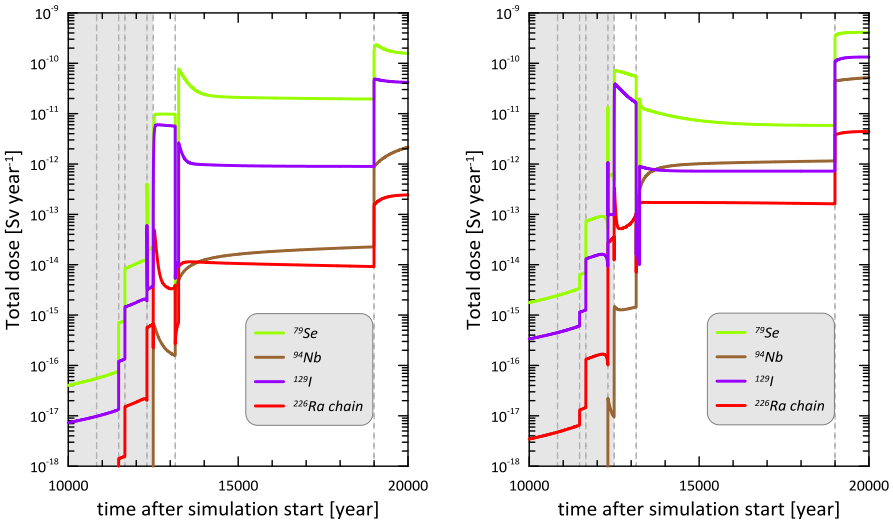

(a) "equal modules" case – the 5-5-5 geometry

(b) "small basin, small agriculture" case – the 5-4-4 geometry

Figure 15: Evolution of doses using the alternatives to the reference basin model – influence of basin geometry on dose. Two alternatives illustrate the influence of variant basin sizes on the evolution of dose, a small basin with equal areas and a smaller basin with smaller agricultural area compared to the Reference case in Figure 13a. The shaded area denotes transitions of Outer and Inner basin ecosystems.

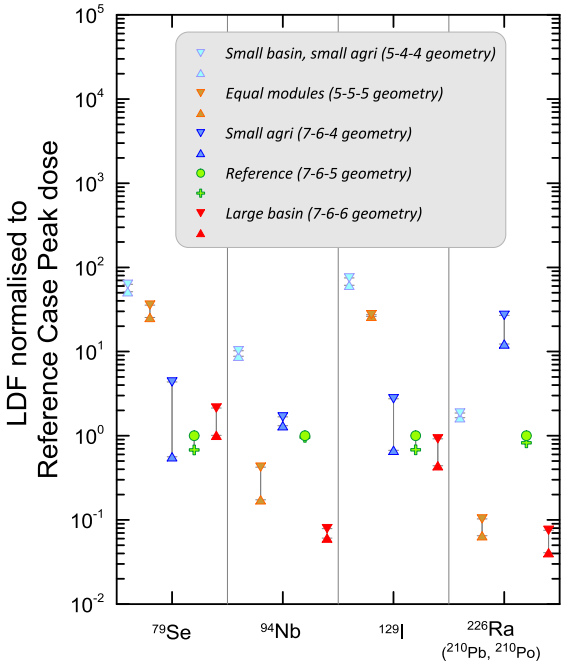

Figure 16: Deterministic sensitivity results for variation of module geometry. Normalised results for four alternative formulations of the basin relative to the 7-6-5 reference geometry.

For the weakly sorbing radionuclides the trends are relatively clear. The larger the basin, the lower the dose. This is the effect of overall water throughput. Spatial dilution is similarly apparent - small basin 5-4-4 geometry gives higher doses than the large basin 7-6-4 case (throughflow) and higher than the 5-5-5 case (spatial dilution). Interestingly, the reference case 7-6-5 geometry gives low results for both ^{79}Se and ^{129}I . This balance between volumetric and spatial dilution mirrors the results of the earlier review by Xu *et al*. (2008).

For the sorbing radionuclides the *lack* of throughflow (collecting area of the whole basin) gives low doses in the 5-5-5 case but high spatial dilution dominates the largest basin case (7-6-6 geometry) with the largest agricultural case considered. The importance of the mobilising effect of throughflow is seen in the prominence of the 7-6-4 basin, especially for the ^{226}Ra chain. This case combines high collecting area with low spatial dilution.

6.5. Use of water resources

As modelled in GEMA-Site there are two potential sources of freshwater for domestic and agricultural purposes. One is the accumulated drainage system water that represents the water that must be diverted from agricultural soils in order to keep them dry enough to cultivate. The other is a shallow well in the lower regolith. One of the variants included in the ranges of Figure 17 is that where well water is also used to irrigate selected crops. During the lake phase, the water source was assumed to be the lake water but during this period there is no agriculture. At the end of the lake period, as the lake becomes clogged with sediment and vegetation and the wetland forms, it is no longer practical to use surface water.

Figure 17: Deterministic sensitivity results for different assumptions about water resource exploitation. Reference case basin (7-6-5 geometry), agricultural transition at 19 kyear.

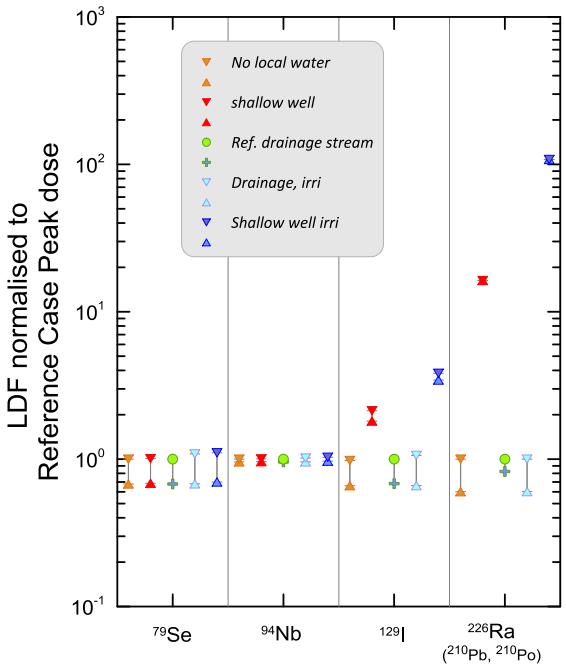

These water use scenarios differ from the SR-Site assumption that drinking water was obtained from a well in the bedrock, the dilution characteristics of which are determined as a regional average figure (Avila et al., 2010). The assumed well capacity is relatively large and contributed to the relatively low drinking water doses in SR-Site (Walke, 2014). In SR-Site water usage from a well was always possible as lakes were assumed always to be present in the landscape. The evolving system implemented in GEMA-Site, with the lake evolving to wetland, would diminish the importance of this scenario. Rather than implement GEMA-Site with the assumed radionuclide concentration in bedrock-well water, a case with no contaminated drinking water has been implemented. In this assumption (which will give doses lower than in the case of the bedrock well) the local population obtain their water resources from uncontaminated sources, for example a lake in a nearby basin or from a public water supply sourced elsewhere in the landscape.

Figure 17 shows an analysis of the impact of different patterns of water usage using the overall maximum and dose post agricultural transition method in the reference case 7-6-5- geometry basin with agricultural transition at 19 kyear.

These results emphasise the need to adequately characterise the habits of the potentially exposed population. For ^{79}Se and ^{94}Nb the assumptions for water usage make little difference, all results are closely clustered around the reference case result. For ^{129}I use of water from the shallow well has a more clearly defined effect, but increasing the dose only by a factor of around two or three if irrigation is included. For the ^{226}Ra chain, however, the results are more important. Because of the relatively high k_d of ^{226}Ra in the lower regolith there is significant accumulation and ingrowth of daughters can lead to over a factor of ten increase relative to the reference (drainage system water used for domestic and agricultural purposes) and no-well-water cases. If the well water is used for irrigation, doses can increase by around two orders of magnitude.

These factors therefore account for a good deal of overall variability and it should be born in mind that Figure 17 does not include the effects of variations in basin geometry discussed above.

6.6. Implications for overall uncertainty

Figure 18 compares the range of uncertainties in estimates of dose using GEMA-Site with the SR-Site LDFs (Avila *et al.*, 2010) and with doses obtained from the application of "simple" biosphere models (Walke, 2014). Differences in the results from the SR-Site radionuclide transport model and GEMA-Site are to be expected – they express alternative interpretations of the groundwater flow systems in the modelled basins. Similarly the “simple” modelling approach carried out by Walke (2014) contributes to the discussion, as an implementation of the "reference biospheres methodology" (IAEA, 2003) applied to the Forsmark site.

In essence the three models used to populate Figure 18 have a great deal in common, though this may not be readily apparent. They all employ the same vertical resolution adopted by Avila *et al*. They each, effectively, treat each basin in the landscape as distinct, recognising that the immediate area around the release point is the most important since most activity entering the biosphere system from the bedrock remains close to the release location. The same exposure pathways are considered in each case. The “complexity” of the SR-site modelling approach comes principally from the modelling of the entire landscape in which ecosystems change in time. The

Figure 18: Uncertainty in results for Basins in the future Forsmark landscape. Results from selected GEMA-Site models are compared with the results from SR-Site (Avila *et al.*, 2010) and an implementation of a "simple" modelling approach (Walke, 2014).

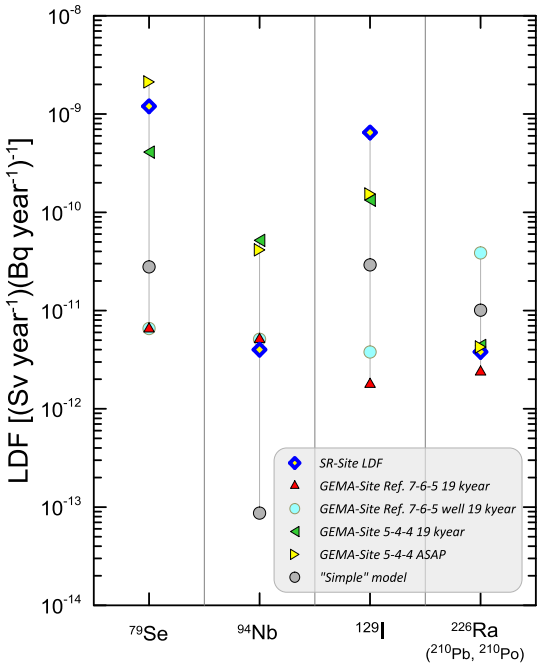

features, events and processes represented in the individual models are all relatively simple, straightforward and robust.

Where the models used here differ from the "standard" approach (eg, the reference biospheres methodology) is that the biosphere system evolves as a consequence of the climate change that brought about the end of the most recent glaciation. Two of the models – SR-Site and GEMA-site encode these changes directly into a coherent structure, resulting in switches that activate changes in the state of the model during the simulation. The "simple" approach uses a set of models that are run independently. The same judgement that the experienced modeller used to implement the "switches" in SR-Site and GEMA-Site are used outside the model execution to combine results in a consistent way. **It is not possible to use off-the-shelf biosphere models without major interpretation to match the specific local conditions set by the site context.** Each of the models applied to the modelling of the future Forsmark landscape is conditioned by the site descriptive modelling that underlies the dose assessment.

Nevertheless, there are differences in the results and these come from two sources, one is the interpretation of the evolution of the site and the other from the assumptions regarding how the exposed population interacts with concentrations of radionuclides in the biosphere. The key feature that GEMA-Site includes is that the groundwater flow vectors change in time in relation to the elevation of the topographic surface relative to sea level.

The time of transition to agriculture reflects how much time the radionuclide release from the bedrock flow system has to accumulate in agricultural soils prior to expo-

sure. In terms of the radiological impact, dose is relatively insensitive to this parameter because it is the maximum dose over the simulation that dictates the dose conversion factor. While it is true that actual doses arising from earlier times would likely be lower than if longer accumulation were possible, this is because the persistence of agricultural land is only a few hundred years at most. As modelled, doses from early conversion would approach the values predicted for later conversion only if agricultural land following early conversion were to exist in the same place until the time assumed for the later conversion.

Basin geometry is a more complex issue. The SKB approach derived a model of the groundwater flow vectors average from six basins at a single time point. This "snapshot" of the flow system was then propagated to provide water fluxes for all basins as a function of time, allowing for evolving areas of wetland and lake. The agricultural ecosystem model was treated separately from the natural ecosystem (accumulation) modelling (see Kłos, 2015). LDFs in SR-Site were taken to be the highest values of dose from releases to each of the basins in the landscape over the whole timespan of the simulation. The duration of the lake phase is short, according to the modelling here (Figure 10). It is not clear that the SKB approach to deriving the flow vectors is sufficient.

A major uncertainty in the modelled basin is the origin of water resources used for domestic and agricultural purposes. Commercial agriculture is less likely to make use of shallow aquifers of questionable quality and reliability. Deep bedrock aquifers are relatively expensive and are less attractive when water supplies from local (other basin) lakes might be available. The simple assumptions in GEMA-Site – use of local water supplies in the form of either well or local drainage system (necessary to maintain viability of agricultural land) can increase doses appreciably, especially when irrigation of crops used for local consumption is carried out.

The "most exposed" group in the local landscape implicit in the GEMA-Site modelling here is a small farm with, potentially, extended family and possibly small community. While irrigation of commercial crops is rare in the present day biosphere, the use of local well water for such a small group in a "kitchen garden" scenario cannot be ruled out. A better characterisation of human habits, activities and lifestyles is needed in future dose assessment applications. There is a balance to be struck between the landscape-defined population group employed by Avila *et al.* (2010) and the traditional subsistence group.

7. Conclusions

The requirement for what became the GEMA-Site model stated that an evolving system featuring different ecosystems should be developed. GEMA-Site has been formulated with reference to one of the basins in the future landscape as a template. It is assumed that the FEPs expressed in this basin are representative of those in alternative configurations expected for other basins in the future landscape, namely, all low-relief lake centred catchments share similar FEPs. The future evolution of basins in the present and future Forsmark landscape involves sea, bay/lake, natural ecosystems (wetland, forest) as well as potential agricultural usage. These have all been implemented in the model, within the limitations of the currently available site description and radionuclide specific database.

Basins are defined by the local topography. Evolution of the site is driven by changes in the water column depth in the basin. Legacy post-glacial landrise is the dominant process. Sedimentation and accumulation of organic matter also plays a role.

The representation of the hydrology of the near-surface regolith changes in response to the evolution and a method – based on mass conservation – has been devised to allow the groundwater vectors in the model of the basin to change significantly depending on the hydrological boundary conditions during the different evolutionary stages. Assuming the FEPs governing the changes in hydrology to be common to all basins in the landscape allows an ensemble of different basins to be represented by varying the geometry of the basin. Basins with different geometry produce significantly different dose results.

GEMA-Site is a *region-specific* model. It takes into account many site-specific details from the SKB site descriptive modelling of the future Forsmark landscape and promotes a flexible model that can be configured to specific basins. There remain some open questions however:

- Mass balance is used to define water fluxes. Most of the water in the biosphere is part of the biosphere and only interacts with the biosphere. Interaction with the geosphere is minimal. Detailed model descriptions of the evolving flow system are available, using *inter alia* the MIKE-SHE model (DHI software, 2009), as employed by SKB. A better means of integrating results from such hydrologic models is desirable.
- Characterisation of human activities is flagged here as important. How the exposed population group uses local water resources is key.
- Agricultural ecosystems dominate dose. For the ^{226}Ra chain, however, the game pathway from natural ecosystems appears to be of high importance. This is, in part, a consequence of the hydrological sub-model of GEMA-Site. The model for exposure via the game consumption pathway needs to be improved.

8. References

Aquilonius K (ed.), 2010. The marine ecosystems at Forsmark and Laxemar-Simpevarp. SR-Site Biosphere. TR-10-03, Svensk Kärnbränslehantering AB.

Avila R, Ekström P-A, Åstrand P-G, 2010. Landscape dose conversion factors used in the safety assessment SR-Site. SKB TR-10-06, Svensk Kärnbränslehantering AB.

Biebighauser TR, 2007. Wetland Drainage, restoration and repair, The University of Kentucky Press, Lexington, Kentucky, USA, 2007

Bosson E., Sassner M., Sabel U., Gustafsson L-G., 2010. Modelling of present and future hydrology and solute transport at Forsmark. SR-Site Biosphere. SKB R-10-02, Svensk Kärnbränslehantering AB.

DHI Software, 2009. MIKE SHE: user manual. DHI Water & Environment, Hørsholm, Denmark, cited by Bosson *et al*., (2010)

Facilia, 2013. http://ecolego.facilia.se/ecolego.

Jansson, U, Kautsky, U and Miliander S, 2006. Rural landscape, production and human consumption: past, present and future. Ambio **35**, No. 8, December 2006

Kłos, RA, 2008. Numerical modelling of SAR-08 biosphere objects, Aleksandria Sciences Project Report to SSM, ASN 08-04, Aleksandria Sciences, United Kingdom

Kłos, RA, 2015, Main phase review - Further modelling and sensitivity study using the GEMA-Site "alternative biosphere models" and review of material from SKB's RFI response, SSM Technical note, in preparation.

Kłos, RA, Shaw, G, Xu, S, Nordén, M, and Wörman, A, 2011. Potential for high transient doses due to accumulation and chemical zonation of long-lived radionuclides across the geosphere-biosphere interface. Radioprotection. 46(6), p453 – p459

Kłos, R A, Limer, L, Shaw, G and Wörman, G, 2012. Initial review phase – Dose Assessment Methodology. SSM Technical Note, Report number 2012:59. ISSN: 2000-0456.

Kłos, RA, and Wörman A, 2013a. Technical note: Initial review phase – Further review of select elements in SKB's Dose Assessment Methodology. Swedish Radiation Safety Authority (SSM2011-592, SSM 2011-4544, 3030007-4033).

Kłos, RA and Wörman, A, 2013b. Uncertainties in doses from agricultural ecosystems following conversion from wetlands. Accepted for presentation at the 2013 International High-Level Radioactive Waste Management Conference, Albuquerque, New Mexico USA, April-May 2013.

Kłos, RA, Limer, L, Shaw, G & Wörman, A, 2014. Modelling comparison of alternative biosphere models with LDF models and evaluation of selected parameter values used in the biosphere dose assessment – Main Review Phase SR-Site, SSM Technical Note, 2014:35, SSM, Stockholm, Sweden.

Lindborg T (ed.), 2010. Landscape Forsmark – data, methodology and results for SR-Site. SKB TR-10-05, Svensk Kärnbränslehantering AB.

Löfgren A (ed), 2010. The terrestrial ecosystems at Forsmark and Laxemar-Simpevarp. SR-Site Biosphere. SKB TR-10-01, Svensk Kärnbränslehantering AB.

Nordén S, Avila R, de la Cruz I, Stenberg K, Grolander S, 2010. Element-specific and constant parameters used for dose calculations in SR-Site. SKB TR-10-07, Svensk Kärnbränslehantering AB.

SKB, 2008. Site description of Forsmark at completion of the site investigation phase SDM-Site Forsmark. SKB Technical Report TR-08-05, Svensk Kärnbränslehantering AB.

SKB, 2010. Climate and climate-related issues for the safety assessment SR-Site. SKB TR-10-49, Svensk Kärnbränslehantering AB.

SKB, 2012. Svar på SSM:s begäran om förtydligande information. SKB DokumentID 1334853.

Smedema LK, Vlotman WF and Rycroft, DW, 2004. Modern Land Drainage: Planning, Design and Management of Agricultural Drainage Systems, AA Balkema, Leiden, Kindle edition, Taylor & Francis, Leiden, ISBN 0-203-02548-2.

SSM, 2008. Strålsäkerhetsmyndigheten föreskrifter och allmänna råd om skydd av människors hälsa och miljön vid slutligt omhändertagande av använt kärnbränsle och kärnavfall. Swedish Radiation Safety Authority Regulatory Code SSMFS 2008:37, Stockholm, ISSN 2000-0987, January 2009.

Walke, R, 2014, Modelling Comparison of Simple Reference Biosphere Models with LDF Models – Main Review Phase, SSM Technical Note 2014:34, Strålsäkerhetsmyndigheten, Stockholm, Sweden, 2014.

Xu, S, Wörman, A, Dverstorp, B, Kłos, RA, Shaw, G & Marklund, L, 2008. SSI's Independent consequence calculations in support of the regulatory review the SR-Can safety assessment, SSI report 2008:08. Statens strålskyddsinstitut, Sweden.

Expressions used in the calculation of dose

This appendix provides a reference for the dose calculations using expressions taken from the Ecolego implementation.

Ingestion pathways

dose_food = H_ing * ing_food * f_aut_food

H_ing	Sv Bq^{-1}	dose per unit intake on ingestion
ing_food	Bq $year^{-1}$	activity intake from ingestion of food at calculated concentration

f_aut_food	-	autarky factor,
		n_food = A_obj / prod_food / I_food
		if (n_food > 1.0) then
		  f_aut_food = 1.0
		else
		  f_aut_food = n_food
		end if

Intake in food

ing_cereal	=	I_cereal*conc_cereal*Zp_cereal	Bq $year^{-1}$
ing_root	=	I_root*conc_root*Zp_root	Bq $year^{-1}$
ing_veg	=	I_veg*conc_veg*Zp_veg	Bq $year^{-1}$
ing_meat	=	I_meat*conc_meat	Bq $year^{-1}$
ing_milk	=	I_milk*conc_milk	Bq $year^{-1}$
ing_crust	=	I_crust*conc_crust*Zp_muscle	Bq $year^{-1}$
ing_fish	=	I_fish*conc_fish*Zp_muscle	Bq $year^{-1}$
ing_berries	=	I_berries*conc_berries / Zp_berries	Bq $year^{-1}$
ing_mush	=	I_mush*conc_mush	Bq $year^{-1}$
ing_game	=	I_game*conc_game*Zp_muscle	Bq $year^{-1}$

Using concentration in the foodstuff as calculated from the concentration in topsoil and water compartments of the model

conc_game	=	CR_game * conc_berries * Zp_berries	Bq kg^{-1} dw
conc_berries	=	If (time < t_colony + t_aqu, 0.0, C_topSoil*CR_natural)	Bq kg^{-1} dw
conc_mush	=	If (time < t_colony + t_aqu, 0.0, C_topSoil*CR_mush)	Bq kg^{-1} dw
conc_crust	=	CentralBasin.water.C_wat*CR_crust	Bq kg^{-1} dw

conc_fish	=	CentralBasin.water.C_wat * if (time < t_sea, CR_fish_sea, CR_fish_fw)	Bq kg^{-1} dw
Conc_crust	=	CentralBasin.water.C_wat * if (time < t_sea, 0.0, CR_crust)	Bq kg^{-1} dw
conc_meat	=	if(time<t_agri, 0.0, (I_beef_wat * C_dw / rho_wat + C_topSoil*I_soil_cattle / n_dpy + C_topSoil * CR_pasture * I_beef_fod * Zp_fodder) * TR_meat)	Bq kg^{-1} fw
conc_milk	=	if(time<t_agri, 0.0, (I_dairy_wat*C_dw / rho_wat + C_topSoil*I_soil_cattle / n_dpy + C_topSoil*CR_pasture*I_dairy_fod*Zp_fodder) * TR_milk)	Bq kg^{-1} fw
conc_cereal	=	if(time<t_agri,0.0, C_topSoil * CR_cereal + (C_irri*n_irri_cereal * lai_cereal * lsc_cereal*irri_retention) / Zp_cereal / prod_cereal)	Bq kg^{-1} fw
conc_root	=	if(time<t_agri,0.0, C_topSoil * CR_root + (C_irri * n_irri_root * lai_root * lsc_root * irri_retention) / Zp_root / prod_root)	Bq kg^{-1} fw
conc_veg	=	if(time<t_agri,0.0, C_topSoil * CR_veg + (C_irri * n_irri_veg * lai_veg * lsc_veg * irri_retention) / Zp_veg / prod_veg)	Bq kg^{-1} fw

The parameter Zp_food is the wet/dry ratio for the foodstuff.

Consumed water concentrations during the evolution are given by:

```
if time < t_aqu
    C_wat = wat / V                ! inventory and volume of water compartment
else
    C_wat = 0.0
end if

if time < t_sea
    C_dw = 0.0                     ! no drinking water during sea stage
else
    if time >= t_agri
        if wellExist
            C_dw = C_low / R       ! well in lower regolith
        else
            C_dw = C_drainage      ! from drainage system
        end if
    else
        C_dw = C_wat               ! surface water compartment (lake)
    end if
    C_irri = C_dw
end if
```

Inhalation dose

dose_inh = H_inh * f_occ * I_air * C_atm

H_inh	Sv Bq^{-1}	dose per unit intake on inhalation
I_air	m^3 $year^{-1}$	Annual inhalation rate
f_occ	year $year^{-1}$	occupancy factor for existing ecosystem
C_atm	Bq m^{-3}	activity concentration in inhaled air:

C_atm = a_dust * C_topSoil

a_dust	kg m^{-3}	airborn dust load

C_topSoil	Bq kg^{-1} dw	concentration in top soil of ecosystem:
		if time < t_agri
		C_natural / (1-epsilon)*rho
		else
		C_agri / (1-epsilon)*rho
		end if
		
		with
		C_natural = upp / V
		C_agri = upp / V
		
		nb, upp is the inventory as a function of time on the compartment. V= V(t) which changes in time and V_agri is not necessarily equal to V_natural.

External dose

dose_ext = H_ext * hpy * f_occ * C_topSoil * (1.0 - epsilon) * rho

H_inh	(Sv $hour^{-1}$)(Bq m^{-3})$^{-1}$	dose per unit intake on inhalation
hpy	hour $year^{-1}$	number of hours each year
f_occ	year $year^{-1}$	occupancy factor for existing ecosystem
C_topSoil	Bq kg^{-1} dw	activity concentration top soil, as above
epsilon	-	porosity of upper regolith
rho	-	grain density of upper regolith

Model implementation of mass balance

The parameterisation of water fluxes in the GEMA-Site reference model requires a translation of the data description of basins in the ~Avila *et al*. (2010) model to match the discretisation of the basin used in GEMA-Site. Figure 19 shows the translation of the water flux data from Bosson *et al*. (2010) as implemented in the Avila *et al*. model for SR-Site, as interpreted by Kłos *et al*. (2014).

As a lake/wetland combination, the situation broadly corresponds to the flow system depicted in Figure 9c. Avila *et al*. model only two distinct areas – at the snapshot of fluxes (based on the interpretation of Bosson *et al*., 2010's "average object") at 5000 CE the wetland (**ter**restrial area) corresponds to the Inner basin and the **aqu**atic area is the lake in the Central basin. The Outer basin is equivalent to the *subcatchment* in the Avila *et al*. description. In the SKB transport model the subcatchment is not described implicitly. Figure 20 is a mass balance check for the Object 116 basin. Setting the numerical values for the water fluxes in this way allows the total water fluxes into the terrestrial and aquatic areas to be evaluated.

To define the parameters for the reference model the expressions

As a snapshot Figure 20 does not directly relate to the evolution of the system. Nevertheless, the fluxes entering the terrestrial part of the "average object" can be used to define the fractional water fluxes from the GEMA-Site Outer basin to the Inner basin during this stage. These parameters are the ϕ_i^{Outer} as discussed on page 26 and defined as

$$\phi_i^{Outer} = \frac{F_{subCatch,i}}{\sum_{i=Low,Mid,Upp} F_{subCatch,i}} \tag{25}$$

where $F_{subCatch,i}$, mm year^{-1}, are the fluxes out the sub-catchment of the "average object". In this way the reference numerical values are:

$$\begin{aligned}
\phi_{Upp}^{Outer} &= \frac{1.8\times10^6}{1.8\times10^6 + 7.4\times10^5 + 5.3\times10^4} = 0.697 \\
\phi_{Mid}^{Outer} &= \frac{7.4\times10^5}{1.8\times10^6 + 7.4\times10^5 + 5.3\times10^4} = 0.282 \\
\phi_{Low}^{Outer} &= 1 - \phi_{Upp}^{Outer} - \phi_{Mid}^{Outer} = \frac{5.3\times10^4}{1.8\times10^6 + 7.4\times10^5 + 5.3\times10^4} = 0.021
\end{aligned} \quad . \tag{26}$$

Water fluxes in the three modules are listed below in Table 8 and the solid material fluxes are set out in Table 9.

Figure 19: Advective transfers as modelled in the radionuclide transport model (Avila et al., 2010). The compartments in the model are shown together with the parameterisation of the fluxes as derived by analysis of Appendix 1 of Avila et al. (2010). This interpretation is taken from Kłos *et al*. (2014).

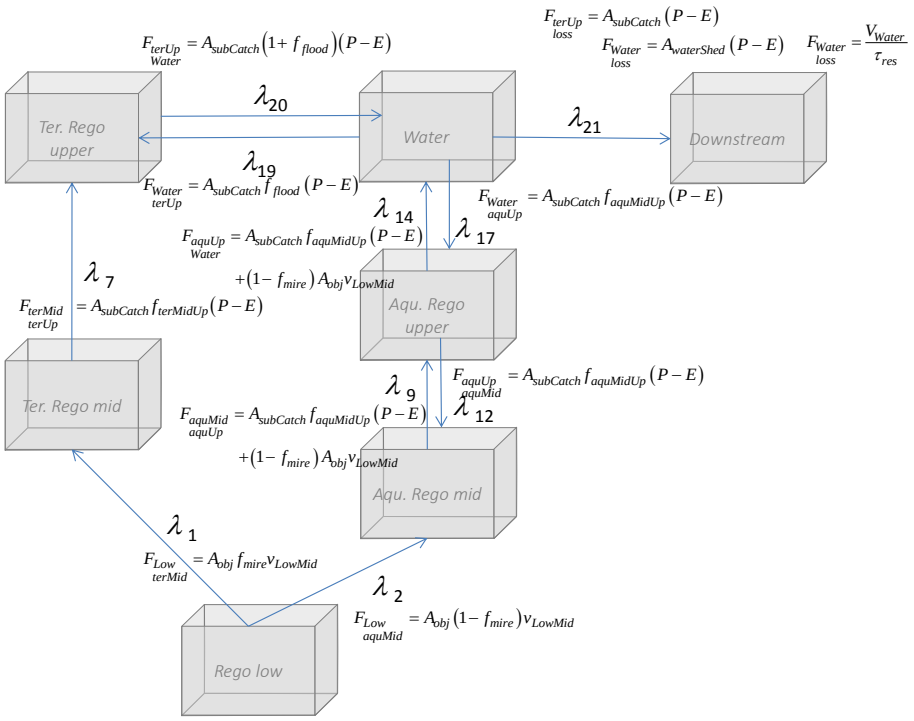

Figure 20. Numerical values for water fluxes in the interpretation of the reference basin (Object 116) using the water flux parameterisation in Figure 19. Fluxes with yellow fill are implied from water balance considerations. Inflows from the subcatchment are used to describe the partitioning of net infiltration in the GEMA-Site Outer basin.

lobj116.ta at 5000	geosphere	subCatch	Low	terMid	terUp	aquMid	aquUp	Water	Down-stream
geosphere			1.6E+04						
subCatch			5.3E+04	7.4E+05	1.8E+06	0.0E+00	0.0E+00	0.0E+00	
Low				6.7E+04		1.4E+03			
terMid					8.1E+05				
terUp								6.0E+06	0.0E+00
aquMid							1.7E+06		
aquUp						1.7E+06		1.7E+06	
Water					3.4E+06		1.7E+06		2.6E+06
Inflow	0	0	6.9E+04	8.0E+05	6.0E+06	1.7E+06	3.4E+06	7.7E+06	2.6E+06
Outflow	1.56E+04	2.61E+06	6.9E+04	8.1E+05	6.0E+06	1.7E+06	3.4E+06	7.7E+06	0.0E+00
Balance	-1.6E+04	-2.6E+06	0.0E+00	-8.9E+03	9.1E+03	0.0E+00	0.0E+00	1.4E+03	2.6E+06

Table 8. Water fluxes in the GEMA-Site modules.

Water fluxes in the Central basin

	Parameter		Ecologo Expression	Outter			Inner			Central			
				t < t_sea	t < t_aqu	t < t_sea	t < t_aqu	t < t_sea	t < t_aqu	t_aqu <= t < t_agri	t >= t_agr
CentralBasin	lower regolith	F_bal	F_bal_out - F_bal_in	0.0	0.0	0.0	0.0	0.0	0.0	0.0	0.0
CentralBasin	lower regolith	F_bal_in	F_tpi + F_bti + F_upi + F_dni	1.0E+03	1.0E+03	3.4E+04	3.4E+04	3.4E+04	3.4E+04	3.4E+04	3.4E+04
CentralBasin	lower regolith	F_bal_out	F_tpo + F_bto + F_upo + F_dno	1.0E+03	1.0E+03	3.4E+04	3.4E+04	3.4E+04	3.4E+04	3.4E+04	3.4E+04
CentralBasin	lower regolith	F_bti	Centralbasin.v_geo*Centralbasin.A_obj	1.0E+03	1.0E+03	1.0E+03	1.0E+03	1.0E+03	1.0E+03	1.0E+03	1.0E+03
CentralBasin	lower regolith	F_bto	0	0.0	0.0	0.0	0.0	0.0	0.0	0.0	0.0
CentralBasin	lower regolith	F_dni	0	0.0	0.0	0.0	0.0	0.0	0.0	0.0	0.0
CentralBasin	lower regolith	F_dno	if(time < Centralbasin.t_aqu, 0.0, 0.0)	0.0	0.0	0.0	0.0	0.0	0.0	0.0	0.0
CentralBasin	lower regolith	F_tpi	if(time < Centralbasin.t_aqu, 0.0, Centralbasin.mid_regolith.F_bto)	0.0	0.0	0.0	0.0	0.0	0.0	0.0	0.0
CentralBasin	lower regolith	F_tpo	if(time < Centralbasin.t_aqu, F_upi + F_bti, F_upi + F_bti)	1.0E+03	1.0E+03	3.4E+04	3.4E+04	3.4E+04	3.4E+04	3.4E+04	3.4E+04
CentralBasin	lower regolith	F_upi	if(time < Outerbasin.t_aqu, 0.0, if(time >=Centralbasin.t_agri, Innerbasin.lower_regolith.F_dno, Innerbasin.lower_regolith.F_dno))	0.0	0.0	3.3E+04	3.3E+04	3.3E+04	3.3E+04	3.3E+04	3.3E+04
CentralBasin	lower regolith	F_upo	0	0.0	0.0	0.0	0.0	0.0	0.0	0.0	0.0
CentralBasin	mid regolith	F_bal	F_bal_out - F_bal_in	0.0	0.0	0.0	0.0	0.0	0.0	0.0	0.0
CentralBasin	mid regolith	F_bal_in	F_tpi + F_bti + F_upi + F_dni	1.0E+03	1.0E+03	3.4E+04	3.4E+04	3.4E+04	3.4E+04	4.9E+05	5.4E+05
CentralBasin	mid regolith	F_bal_out	F_tpo + F_bto + F_upo + F_dno	1.0E+03	1.0E+03	3.4E+04	3.4E+04	3.4E+04	3.4E+04	4.9E+05	5.4E+05
CentralBasin	mid regolith	F_bti	if(time < Centralbasin.t_aqu, Centralbasin.lower_regolith.F_tpo, Centralbasin.lower_regolith.F_tpo)	1.0E+03	1.0E+03	3.4E+04	3.4E+04	3.4E+04	3.4E+04	3.4E+04	3.4E+04
CentralBasin	mid regolith	F_bto	if(time < Centralbasin.t_aqu, 0.0, 0.0)	0.0	0.0	0.0	0.0	0.0	0.0	0.0	0.0
CentralBasin	mid regolith	F_dni	0	0.0	0.0	0.0	0.0	0.0	0.0	0.0	0.0
CentralBasin	mid regolith	F_dno	if(time < Centralbasin.t_aqu, 0.0, if(time >=Centralbasin.t_agri, F_upi + F_tpi + F_bti - F_tpo, 0.0))	0.0	0.0	0.0	0.0	0.0	0.0	0.0	5.0E+05
CentralBasin	mid regolith	F_tpi	if(time < Centralbasin.t_aqu, 0.0, Centralbasin.upper_regolith.F_bto)	0.0	0.0	0.0	0.0	0.0	0.0	0.0	5.6E+04
CentralBasin	mid regolith	F_tpo	if(time < Centralbasin.t_aqu, F_bti + F_upi, if(time >=Centralbasin.t_agri, ETp*Centralbasin.A_obj, F_bti + F_upi))	1.0E+03	1.0E+03	3.4E+04	3.4E+04	3.4E+04	4.9E+05	4.0E+04	
CentralBasin	mid regolith	F_upi	if(time < Outerbasin.t_aqu, 0.0, Innerbasin.mid_regolith.F_dno)	0.0	0.0	0.0	0.0	0.0	0.0	4.5E+05	4.5E+05
CentralBasin	mid regolith	F_upo	0	0.0	0.0	0.0	0.0	0.0	0.0	0.0	0.0

Table 8. Water fluxes in the GEMA-Site modules. (Continued).

Water fluxes in the Central basin (continued)

	Parameter		Ecolego Expression	Outer		Inner		Central		
				t < t_sea	t < t_aqu	t < t_sea	t < t_aqu	t < t_sea	t < t_aqu	t_aqu <= t < t_agri	t >= t_agr
CentralBasin	upper regolith	F_bal	F_bal_out - F_bal_in	0.0	0.0	0.0	0.0	0.0	0.0	0.0	0.0
CentralBasin	upper regolith	F_bal_in	F_tpi + F_bti + F_upi + F_dni	1.0E+03	1.0E+03	3.4E+04	3.4E+04	3.4E+04	1.8E+06	9.6E+04	
CentralBasin	upper regolith	F_bal_out	F_tpo + F_bto + F_upo + F_dno	1.0E+03	1.0E+03	3.4E+04	3.4E+04	3.4E+04	1.8E+06	9.6E+04	
CentralBasin	upper regolith	F_bti	Centralbasin.mid_regolith.F_tpo	1.0E+03	1.0E+03	3.4E+04	3.4E+04	3.4E+04	4.9E+05	4.0E+04	
CentralBasin	upper regolith	F_bto	if(time < Centralbasin.t_aqu, 0.0, if(time >=Centralbasin.t_agri, F_tpi, 0.0))	0.0	0.0	0.0	0.0	0.0	0.0	5.6E+04	
CentralBasin	upper regolith	F_dni	0	0.0	0.0	0.0	0.0	0.0	0.0	0.0	
CentralBasin	upper regolith	F_dno	if(time < Centralbasin.t_aqu, 0.0, if(time >=Centralbasin.t_agri, 0.0, F_tpi - F_tpo + F_upi + F_bti))	0.0	0.0	0.0	0.0	0.0	1.8E+06	0.0	
CentralBasin	upper regolith	F_tpi	if(time < Centralbasin.t_aqu, 0.0, Ppt*Centralbasin.A_obj + Centralbasin.F_irri - Centralbasin.F_intercept)	0.0	0.0	0.0	0.0	0.0	5.6E+04	5.6E+04	
CentralBasin	upper regolith	F_tpo	if(time < Centralbasin.t_aqu, F_bti + F_upi, ETp*Centralbasin.A_obj)	1.0E+03	1.0E+03	3.4E+04	3.4E+04	3.4E+04	4.0E+04	4.0E+04	
CentralBasin	upper regolith	F_upi	if(time < Outerbasin.t_aqu, 0.0, if(time >=Centralbasin.t_agri, 0.0, Innerbasin.upper_regolith.F_dno))	0.0	0.0	0.0	0.0	0.0	1.3E+06	0.0	
CentralBasin	upper regolith	F_upo	0	0.0	0.0	0.0	0.0	0.0	0.0	0.0	
CentralBasin	water	F_bal	F_bal_out - F_bal_in	0.0	0.0	0.0	0.0	0.0	0.0	0.0	
CentralBasin	water	F_bal_in	F_tpi + F_bti + F_upi + F_dni	9.4E+08	9.4E+08	9.4E+08	9.4E+08	9.4E+08	5.6E+04	0.0	
CentralBasin	water	F_bal_out	F_tpo + F_bto + F_upo + F_dno	9.4E+08	9.4E+08	9.4E+08	9.4E+08	9.4E+08	5.6E+04	0.0	
CentralBasin	water	F_bti	if(time < Centralbasin.t_aqu, Centralbasin.upper_regolith.F_tpo, 0.0)	1.0E+03	1.0E+03	3.4E+04	3.4E+04	3.4E+04	0.0	0.0	
CentralBasin	water	F_bto	0	0.0	0.0	0.0	0.0	0.0	0.0	0.0	
CentralBasin	water	F_dni	F_dno - (F_tpi - F_tpo) - F_bti	4.7E+08	4.7E+08	4.7E+08	4.7E+08	4.7E+08	0.0	0.0	
CentralBasin	water	F_dno	if(time < Centralbasin.t_aqu, F_upi + F_bti + F_tpi - F_tpo, 0.0)	4.7E+08	4.7E+08	4.7E+08	4.7E+08	4.7E+08	1.6E+04	0.0	
CentralBasin	water	F_tpi	if(time < Centralbasin.t_aqu, Ppt*Centralbasin.A_obj, 0.0)	5.6E+04	5.6E+04	5.6E+04	5.6E+04	5.6E+04	5.6E+04	0.0	
CentralBasin	water	F_tpo	if(time < Centralbasin.t_aqu, ETp*Centralbasin.A_obj, 0.0)	4.0E+04	4.0E+04	4.0E+04	4.0E+04	4.0E+04	4.0E+04	0.0	
CentralBasin	water	F_upi	if(time <=Centralbasin.t_sea, Centralbasin.A_obj*(1/tau_wat_ret - Centralbasin.v_geo - (Ppt - ETp)), 0.0)	4.7E+08	4.7E+08	4.7E+08	4.7E+08	4.7E+08	0.0	0.0	
CentralBasin	water	F_upo	if(time <=Centralbasin.t_sea, Centralbasin.A_obj*(1/tau_wat_ret - Centralbasin.v_geo - (Ppt - ETp)), 0.0)	4.7E+08	4.7E+08	4.7E+08	4.7E+08	4.7E+08	0.0	0.0	
CentralBasin		F_intercept	if(time < t_agri, 0.0, (n_irri_cereal*lai_cereal*lsc_cereal*area_cereal) + (n_irri_root*lai_root*lsc_root*area_root) + (n_irri_veg*lai_veg*lsc_veg*area_veg))	0.0	0.0	0.0	0.0	0.0	0.0	0.0	
CentralBasin		F_irri	if(time < t_agri, 0.0, (n_irri_cereal*l_irri_cereal*area_cereal) + (n_irri_veg*l_irri_veg*area_veg) + (n_irri_root*l_irri_root*area_root))	0.0	0.0	0.0	0.0	0.0	0.0	0.0	0.0

Table 8. Water fluxes in the GEMA-Site modules. (Continued).

Water fluxes in the Inner basin

				Outer		Inner		Central			
	Parameter		Ecolego Expression	t < t_sea	t < t_aqu	t < t_sea	t < t_aqu	t < t_sea	t < t_aqu	t_aqu <= t < t_agri	t >= t_agr
InnerBasin	lower regolith	F_bal	F_bal_out - F_bal_in	0.0	0.0	0.0	0.0	0.0	0.0	0.0	0.0
InnerBasin	lower regolith	F_bal_in	F_tpi + F_bti + F_upi + F_dni	0.0	0.0	3.3E+04	3.3E+04	3.3E+04	3.3E+04	3.3E+04	3.3E+04
InnerBasin	lower regolith	F_bal_out	F_tpo + F_bto + F_upo + F_dno	0.0	0.0	3.3E+04	3.3E+04	3.3E+04	3.3E+04	3.3E+04	3.3E+04
InnerBasin	lower regolith	F_bti	Innerbasin.v_geo*Innerbasin.A_obj	0.0	0.0	0.0	0.0	0.0	0.0	0.0	0.0
InnerBasin	lower regolith	F_bto	0	0.0	0.0	0.0	0.0	0.0	0.0	0.0	0.0
InnerBasin	lower regolith	F_dni	0	0.0	0.0	0.0	0.0	0.0	0.0	0.0	0.0
InnerBasin	lower regolith	F_dno	if(time < Innerbasin.t_aqu, 0.0, F_upi + F_bti + F_tpi - Innerbasin.F_irri)	0.0	0.0	3.3E+04	3.3E+04	3.3E+04	3.3E+04	3.3E+04	3.3E+04
InnerBasin	lower regolith	F_tpi	if(time < Innerbasin.t_aqu, 0.0, Innerbasin.mid_regolith.F_bto)	0.0	0.0	0.0	0.0	0.0	0.0	0.0	0.0
InnerBasin	lower regolith	F_tpo	if(time < Innerbasin.t_aqu, F_upi + F_bti, if(time < Centralbasin.t_aqu, 0.0, 0.0))	0.0	3.3E+04	0.0	0.0	0.0	0.0	0.0	0.0
InnerBasin	lower regolith	F_upi	if(time < Outerbasin.t_aqu, 0.0, if(time >=Innerbasin.t_agri, Outerbasin.lower_regolith.F_dno), Outerbasin.lower_regolith.F_dno))	0.0	3.3E+04	3.3E+04	3.3E+04	3.3E+04	3.3E+04	3.3E+04	3.3E+04
InnerBasin	lower regolith	F_upo	0	0.0	0.0	0.0	0.0	0.0	0.0	0.0	0.0
InnerBasin	upper regolith	F_bal	F_bal_out - F_bal_in	0.0	0.0	0.0	0.0	0.0	0.0	0.0	0.0
InnerBasin	upper regolith	F_bal_in	F_tpi + F_bti + F_upi + F_dni	0.0	4.8E+05	2.1E+06	2.1E+06	1.7E+06	1.7E+06	1.7E+06	1.7E+06
InnerBasin	upper regolith	F_bal_out	F_tpo + F_bto + F_upo + F_dno	0.0	4.8E+05	2.1E+06	2.1E+06	1.7E+06	1.7E+06	1.7E+06	1.7E+06
InnerBasin	upper regolith	F_bti	Innerbasin.mid_regolith.F_tpo	0.0	4.8E+05	4.5E+05	4.5E+05	0.0	0.0	0.0	0.0
InnerBasin	upper regolith	F_bto	if(time < Innerbasin.t_aqu, 0.0, if(time >=Innerbasin.t_agri, F_tpi - F_bti, 0.0))	0.0	0.0	0.0	0.0	0.0	0.0	0.0	0.0
InnerBasin	upper regolith	F_dni	0	0.0	0.0	0.0	0.0	0.0	0.0	0.0	0.0
InnerBasin	upper regolith	F_dno	if(time < Innerbasin.t_aqu, 0.0, if(time >=Innerbasin.t_agri, 0.0, F_tpi - F_tpo + F_upi + F_bti))	0.0	0.0	1.7E+06	1.7E+06	1.3E+06	1.3E+06	1.3E+06	1.3E+06
InnerBasin	upper regolith	F_tpi	if(time < Innerbasin.t_aqu, 0.0, Ppt*Innerbasin.A_obj + Innerbasin.F_irri - Innerbasin.F_intercept)	0.0	0.0	5.6E+05	5.6E+05	5.6E+05	5.6E+05	5.6E+05	5.6E+05
InnerBasin	upper regolith	F_tpo	if(time < Innerbasin.t_aqu, F_bti + F_upi, ETp*Innerbasin.A_obj)	0.0	4.8E+05	4.0E+05	4.0E+05	4.0E+05	4.0E+05	4.0E+05	4.0E+05
InnerBasin	upper regolith	F_upi	if(time < Outerbasin.t_aqu, 0.0, if(time >=Innerbasin.t_agri, 0.0, Outerbasin.upper_regolith.F_dno))	0.0	0.0	1.1E+06	1.1E+06	1.1E+06	1.1E+06	1.1E+06	1.1E+06
InnerBasin	upper regolith	F_upo	0	0.0	0.0	0.0	0.0	0.0	0.0	0.0	0.0
InnerBasin	water	F_bal	F_bal_out - F_bal_in	0.0	0.0	0.0	0.0	0.0	0.0	0.0	0.0
InnerBasin	water	F_bal_in	F_tpi + F_bti + F_upi + F_dni	8.8E+09	8.8E+09	9.6E+05	0.0	0.0	0.0	0.0	0.0
InnerBasin	water	F_bal_out	F_tpo + F_bto + F_upo + F_dno	8.8E+09	8.8E+09	9.6E+05	0.0	0.0	0.0	0.0	0.0

Table 8. Water fluxes in the GEMA-Site modules. (Continued).

Water fluxes in the Inner basin (continued)

				Outer			Inner			Central		
	Parameter		Ecolego Expression	t < t_sea	t < t_aqu	t < t_sea	t < t_aqu	t < t_sea	t < t_aqu	t_aqu <= t < t_agri	t >= t_agr
InnerBasin	water	F_bal	F_bal_out - F_bal_in	0.0	0.0	0.0	0.0	0.0	0.0	0.0	0.0
InnerBasin	water	F_bal_in	F_tpi + F_bti + F_upi + F_dni	8.8E+09	8.8E+09	9.6E+05		0.0	0.0	0.0	0.0
InnerBasin	water	F_bal_out	F_tpo + F_bto + F_upo + F_dno	8.8E+09	8.8E+09	9.6E+05		0.0	0.0	0.0	0.0
InnerBasin	upper regolith	F_bti	Innerbasin.mid_regolith.F_tpo	0.0	0.0	4.8E+05	4.5E+05	4.5E+05	0.0	0.0	0.0
InnerBasin	upper regolith	F_bto	if(time < Innerbasin.t_aqu, 0.0, if(time >=Innerbasin.t_agri, F_tpi - F_bti, 0.0))	0.0	0.0	0.0	0.0	0.0	0.0	0.0	0.0
InnerBasin	upper regolith	F_dni	0	0.0	0.0	0.0	0.0	0.0	0.0	0.0	0.0
InnerBasin	upper regolith	F_dno	if(time < Innerbasin.t_aqu, 0.0, if(time >=Innerbasin.t_agri, 0.0, F_tpi - F_tpo + F_upi + F_bti))	0.0	0.0	0.0	1.7E+06	1.7E+06	1.3E+06	1.3E+06	1.3E+06
InnerBasin	upper regolith	F_tpi	if(time < Innerbasin.t_aqu, 0.0, Ppt*Innerbasin.A_obj + Innerbasin.F_irri - Innerbasin.F_intercept)	0.0	0.0	0.0	5.6E+05	5.6E+05	5.6E+05	5.6E+05	5.6E+05
InnerBasin	upper regolith	F_tpo	if(time < Innerbasin.t_aqu, F_bti + F_upi, ETp*Innerbasin.A_obj)	0.0	0.0	4.8E+05	4.0E+05	4.0E+05	4.0E+05	4.0E+05	4.0E+05
InnerBasin	upper regolith	F_upi	if(time < Outerbasin.t_aqu, 0.0, if(time >=Innerbasin.t_agri, 0.0, Outerbasin.upper_regolith.F_dno))	0.0	0.0	0.0	1.1E+06	1.1E+06	1.1E+06	1.1E+06	1.1E+06
InnerBasin	upper regolith	F_upo	0	0.0	0.0	0.0	0.0	0.0	0.0	0.0	0.0
InnerBasin	water	F_bal	F_bal_out - F_bal_in	0.0	0.0	0.0	0.0	0.0	0.0	0.0	0.0
InnerBasin	water	F_bal_in	F_tpi + F_bti + F_upi + F_dni	8.8E+09	8.8E+09	8.8E+09	9.6E+05	0.0	0.0	0.0	0.0
InnerBasin	water	F_bal_out	F_tpo + F_bto + F_upo + F_dno	8.8E+09	8.8E+09	8.8E+09	9.6E+05	0.0	0.0	0.0	0.0
InnerBasin	water	F_bti	if(time < Innerbasin.t_aqu, Innerbasin.upper_regolith.F_tpo, 0.0)	0.0	0.0	4.8E+05	4.0E+05	0.0	0.0	0.0	0.0
InnerBasin	water	F_bto	0	0.0	0.0	0.0	0.0	0.0	0.0	0.0	0.0
InnerBasin	water	F_dni	if(time < Innerbasin.t_sea, F_dno - (F_tpi - F_tpo) - F_bti, 0.0)	4.4E+09	4.4E+09	4.4E+09	0.0	0.0	0.0	0.0	0.0
InnerBasin	water	F_dno	if(time < Innerbasin.t_aqu, F_upi + F_bti + F_tpi - F_tpo, 0.0)	4.4E+09	4.4E+09	4.4E+09	5.6E+05	0.0	0.0	0.0	0.0
InnerBasin	water	F_tpi	if(time < Innerbasin.t_aqu, Ppt*Innerbasin.A_obj, 0.0)	5.6E+05	5.6E+05	5.6E+05	5.6E+05	0.0	0.0	0.0	0.0
InnerBasin	water	F_tpo	if(time < Innerbasin.t_aqu, ETp*Innerbasin.A_obj, 0.0)	4.0E+05	4.0E+05	4.0E+05	4.0E+05	0.0	0.0	0.0	0.0
InnerBasin	water	F_upi	if(time <=Innerbasin.t_sea, Innerbasin.A_obj*(1/tau_wat_ret - Innerbasin.v_geo - (Ppt - ETp)), 0.0)	4.4E+09	4.4E+09	4.4E+09	0.0	0.0	0.0	0.0	0.0
InnerBasin	water	F_upo	if(time <=Innerbasin.t_sea, Innerbasin.A_obj*(1/tau_wat_ret - Innerbasin.v_geo - (Ppt - ETp)), 0.0)	4.4E+09	4.4E+09	4.4E+09	0.0	0.0	0.0	0.0	0.0
InnerBasin		F_intercept	if(time < t_agri, 0.0, (n_irri_cereal*lai_cereal*lsc_cereal*area_cereal) + (n_irri_root*lai_root*lsc_root*area_root) + (n_irri_veg*lai_veg*lsc_veg*area_veg))	0.0	0.0	0.0	0.0	0.0	0.0	0.0	0.0
InnerBasin		F_irri	if(time < t_agri, 0.0, (n_irri_cereal*l_irri_cereal*area_cereal) + (n_irri_veg*l_irri_veg*area_veg) + (n_irri_root*l_irri_root*area_root))	0.0	0.0	0.0	0.0	0.0	0.0	0.0	0.0

Table 8. Water fluxes in the GEMA-Site modules. (Continued).

Water fluxes in the Outer basin

				Outer		Inner		Central			
	Parameter		Ecolego Expression	t < t_sea	t < t_aqu	t < t_sea	t < t_aqu	t < t_sea	t < t_aqu	t_aqu <= t < t_agri	t >= t_agr
OuterBasin	lower regolith	F_bal	F_bal_out - F_bal_in	0.0E+00	0.0E+00	0.0E+00	0.0E+00	0.0E+00	0.0E+00	0.0E+00	0.0E+00
OuterBasin	lower regolith	F_bal_in	F_tpi + F_bti + F_upi + F_dni	0.0E+00	0.0E+00	3.3E+04	3.3E+04	3.3E+04	3.3E+04	3.3E+04	3.3E+04
OuterBasin	lower regolith	F_bal_out	F_tpo + F_bto + F_upo + F_dno	0.0E+00	0.0E+00	3.3E+04	3.3E+04	3.3E+04	3.3E+04	3.3E+04	3.3E+04
OuterBasin	lower regolith	F_bti	Outerbasin.v_geo*Outerbasin.A_obj	0.0E+00	0.0E+00	0.0E+00	0.0E+00	0.0E+00	0.0E+00	0.0E+00	0.0E+00
OuterBasin	lower regolith	F_bto	0	0.0E+00	0.0E+00	0.0E+00	0.0E+00	0.0E+00	0.0E+00	0.0E+00	0.0E+00
OuterBasin	lower regolith	F_dni	0	0.0E+00	0.0E+00	0.0E+00	0.0E+00	0.0E+00	0.0E+00	0.0E+00	0.0E+00
OuterBasin	lower regolith	F_dno	if(time < Outerbasin.t_aqu, 0.0, F_bti + F_tpi - Outerbasin.F_irri)	0.0E+00	0.0E+00	3.3E+04	3.3E+04	3.3E+04	3.3E+04	3.3E+04	3.3E+04
OuterBasin	lower regolith	F_tpi	if(time < Outerbasin.t_aqu, 0.0, Outerbasin.mid_regolith.F_bto)	0.0E+00	0.0E+00	3.3E+04	3.3E+04	3.3E+04	3.3E+04	3.3E+04	3.3E+04
OuterBasin	lower regolith	F_tpo	if(time < Outerbasin.t_aqu, F_bti, 0.0)	0.0E+00	0.0E+00	0.0E+00	0.0E+00	0.0E+00	0.0E+00	0.0E+00	0.0E+00
OuterBasin	lower regolith	F_upi	0	0.0E+00	0.0E+00	0.0E+00	0.0E+00	0.0E+00	0.0E+00	0.0E+00	0.0E+00
OuterBasin	lower regolith	F_upo	0	0.0E+00	0.0E+00	0.0E+00	0.0E+00	0.0E+00	0.0E+00	0.0E+00	0.0E+00
OuterBasin	upper regolith	F_bal	F_bal_out - F_bal_in	0.0E+00	0.0E+00	0.0E+00	0.0E+00	0.0E+00	0.0E+00	0.0E+00	0.0E+00
OuterBasin	upper regolith	F_bal_in	F_tpi + F_bti + F_upi + F_dni	0.0E+00	0.0E+00	4.8E+05	4.8E+05	4.8E+05	4.8E+05	4.8E+05	4.8E+05
OuterBasin	upper regolith	F_bal_out	F_tpo + F_bto + F_upo + F_dno	0.0E+00	0.0E+00	4.8E+05	4.8E+05	4.8E+05	4.8E+05	4.8E+05	4.8E+05
OuterBasin	upper regolith	F_bti	if(time < Outerbasin.t_aqu, Outerbasin.lower_regolith.F_tpo, 0.0)	0.0E+00	0.0E+00	0.0E+00	0.0E+00	0.0E+00	0.0E+00	0.0E+00	0.0E+00
OuterBasin	upper regolith	F_bto	if(time < Outerbasin.t_aqu, 0.0, F_tpi - F_dno)	0.0E+00	0.0E+00	3.3E+04	3.3E+04	3.3E+04	3.3E+04	3.3E+04	3.3E+04
OuterBasin	upper regolith	F_dni	0	0.0E+00	0.0E+00	0.0E+00	0.0E+00	0.0E+00	0.0E+00	0.0E+00	0.0E+00
OuterBasin	upper regolith	F_dno	if(time < Outerbasin.t_aqu, 0.0, Outerbasin.phi_mid*(Outerbasin.upper_regolith.F_tpi - Outerbasin.upper_regolith.F_tpo))	0.0E+00	0.0E+00	4.5E+05	4.5E+05	4.5E+05	4.5E+05	4.5E+05	4.5E+05
OuterBasin	upper regolith	F_tpi	if(time < Outerbasin.t_aqu, 0.0, Outerbasin.upper_regolith.F_bto)	0.0E+00	0.0E+00	4.8E+05	4.8E+05	4.8E+05	4.8E+05	4.8E+05	4.8E+05
OuterBasin	upper regolith	F_tpo	if(time < Outerbasin.t_aqu, F_bti, 0.0)	0.0E+00	0.0E+00	0.0E+00	0.0E+00	0.0E+00	0.0E+00	0.0E+00	0.0E+00
OuterBasin	upper regolith	F_upi	0	0.0E+00	0.0E+00	0.0E+00	0.0E+00	0.0E+00	0.0E+00	0.0E+00	0.0E+00
OuterBasin	upper regolith	F_upo	0	0.0E+00	0.0E+00	0.0E+00	0.0E+00	0.0E+00	0.0E+00	0.0E+00	0.0E+00

Table 8. Water fluxes in the GEMA-Site modules. (Continued).

Water fluxes in the Outer basin (continued)

				Outer		Inner		Central			
	Parameter		Ecolego Expression	t < t_sea	t < t_aqu	t < t_sea	t < t_aqu	t < t_sea	t < t_aqu	t_aqu <= t < t_agri	t >= t_agr
OuterBasin	water	F_bal	F_bal_out - F_bal_in	0.0E+00	0.0E+00	0.0E+00	0.0E+00	0.0E+00	0.0E+00	0.0E+00	0.0E+00
OuterBasin	water	F_bal_in	F_tpi + F_bti + F_upi + F_dni	0.0E+00	0.0E+00	5.6E+06	5.6E+06	5.6E+06	5.6E+06	5.6E+06	5.6E+06
OuterBasin	water	F_bal_out	F_tpo + F_bto + F_upo + F_dno	0.0E+00	0.0E+00	5.6E+06	5.6E+06	5.6E+06	5.6E+06	5.6E+06	5.6E+06
OuterBasin	upper regolith	F_bti	if(time < Outerbasin.t_aqu, Outerbasin.mid_regolith.F_tpo, 0.0)	0.0E+00	0.0E+00	0.0E+00	0.0E+00	0.0E+00	0.0E+00	0.0E+00	0.0E+00
OuterBasin	upper regolith	F_bto	if(time < Outerbasin.t_aqu, 0.0, (1.0 - Outerbasin.phi_upp)*(F_tpi - F_tpo))	0.0E+00	0.0E+00	4.8E+05	4.8E+05	4.8E+05	4.8E+05	4.8E+05	4.8E+05
OuterBasin	upper regolith	F_dni	0	0.0E+00	0.0E+00	0.0E+00	0.0E+00	0.0E+00	0.0E+00	0.0E+00	0.0E+00
OuterBasin	upper regolith	F_dno	if(time < Outerbasin.t_aqu, 0.0, Outerbasin.phi_upp*(F_tpi - F_tpo))	0.0E+00	0.0E+00	1.1E+06	1.1E+06	1.1E+06	1.1E+06	1.1E+06	1.1E+06
OuterBasin	upper regolith	F_tpi	if(time < Outerbasin.t_aqu, 0.0, Ppt*Outerbasin.A_obj + Outerbasin.F_irri - Outerbasin.F_intercept)	0.0E+00	0.0E+00	5.6E+06	5.6E+06	5.6E+06	5.6E+06	5.6E+06	5.6E+06
OuterBasin	upper regolith	F_tpo	if(time < Outerbasin.t_aqu, F_bti, ETp*Outerbasin.A_obj)	0.0E+00	0.0E+00	4.0E+06	4.0E+06	4.0E+06	4.0E+06	4.0E+06	4.0E+06
OuterBasin	upper regolith	F_upi	0	0.0E+00	0.0E+00	0.0E+00	0.0E+00	0.0E+00	0.0E+00	0.0E+00	0.0E+00
OuterBasin	upper regolith	F_upo	0	0.0E+00	0.0E+00	0.0E+00	0.0E+00	0.0E+00	0.0E+00	0.0E+00	0.0E+00
OuterBasin	water	F_bal	if(time < Outerbasin.t_aqu, Outerbasin.mid_regolith.F_tpo, 0.0)	0.0E+00	0.0E+00	0.0E+00	0.0E+00	0.0E+00	0.0E+00	0.0E+00	0.0E+00
OuterBasin	water	F_bal_in	if(time < Outerbasin.t_aqu, 0.0, (1.0 - Outerbasin.phi_upp)*(F_tpi - F_tpo))	0.0E+00	0.0E+00	4.8E+05	4.8E+05	4.8E+05	4.8E+05	4.8E+05	4.8E+05
OuterBasin	water	F_bal_out	0	0.0E+00	0.0E+00	0.0E+00	0.0E+00	0.0E+00	0.0E+00	0.0E+00	0.0E+00
OuterBasin	water	F_bti	F_bal_out - F_bal_in	0.0E+00	0.0E+00	0.0E+00	0.0E+00	0.0E+00	0.0E+00	0.0E+00	0.0E+00
OuterBasin	water	F_bto	F_tpi + F_bti + F_upi + F_dni	4.5E+10	5.6E+06	0.0E+00	0.0E+00	0.0E+00	0.0E+00	0.0E+00	0.0E+00
OuterBasin	water	F_dni	F_tpo + F_bto + F_upo + F_dno	4.5E+10	5.6E+06	0.0E+00	0.0E+00	0.0E+00	0.0E+00	0.0E+00	0.0E+00
OuterBasin	water	F_dno	if(time < Outerbasin.t_aqu, Outerbasin.upper_regolith.F_tpo, 0.0)	0.0E+00	0.0E+00	0.0E+00	0.0E+00	0.0E+00	0.0E+00	0.0E+00	0.0E+00
OuterBasin	water	F_tpi	0	0.0E+00	0.0E+00	0.0E+00	0.0E+00	0.0E+00	0.0E+00	0.0E+00	0.0E+00
OuterBasin	water	F_tpo	F_dno - (F_tpi - F_tpo)	4.1E+09	0.0E+00	0.0E+00	0.0E+00	0.0E+00	0.0E+00	0.0E+00	0.0E+00
OuterBasin	water	F_upi	if(time <=Innerbasin.t_sea, Innerbasin.A_obj*(1/tau_wat_ret - Innerbasin.v_geo - (Ppt - ETp)), 0.0)	4.1E+09	1.6E+06	0.0E+00	0.0E+00	0.0E+00	0.0E+00	0.0E+00	0.0E+00
OuterBasin	water	F_upo	if(time < Outerbasin.t_aqu, Ppt*Outerbasin.A_obj, 0.0)	5.6E+06	5.6E+06	0.0E+00	0.0E+00	0.0E+00	0.0E+00	0.0E+00	0.0E+00
OuterBasin		F_intercept	if(time < Outerbasin.t_aqu, ETp*Outerbasin.A_obj, 0.0)	4.0E+06	4.0E+06	0.0E+00	0.0E+00	0.0E+00	0.0E+00	0.0E+00	0.0E+00
OuterBasin		F_irri	if(time <=Outerbasin.t_sea, Outerbasin.A_obj*(1/tau_wat_ret - Outerbasin.v_geo - (Ppt - ETp)), 0.0)	4.1E+10	0.0E+00	0.0E+00	0.0E+00	0.0E+00	0.0E+00	0.0E+00	0.0E+00

Parameter			expression
Central	water	M_bti	if(time < CentralBasin.t_aqu, CentralBasin.sed_upp*CentralBasin.A_obj, 0.0)
	water	M_bto	if(time < CentralBasin.t_aqu, CentralBasin.sed_ned*CentralBasin.A_obj, 0.0)
	Upper regolith	M_tpi	if(time < CentralBasin.t_aqu, CentralBasin.water.M_bto, 0.0)
	Upper regolith	M_tpo	if(time < CentralBasin.t_aqu, CentralBasin.water.M_bti, 0.0)
Inner	Water	M_bti	if(time < InnerBasin.t_aqu, InnerBasin.sed_upp*InnerBasin.A_obj, 0.0)
	Water	M_bto	if(time < InnerBasin.t_aqu, InnerBasin.sed_ned*InnerBasin.A_obj, 0.0)
	Upper regolith	M_tpi	if(time < InnerBasin.t_aqu, InnerBasin.water.M_bto, 0.0)
	Upper regolith	M_tpo	if(time < InnerBasin.t_aqu, InnerBasin.water.M_bti, 0.0)
Outer	Water	M_bti	if(time < OuterBasin.t_aqu, OuterBasin.sed_upp*OuterBasin.A_obj, 0.0)
	Water	M_bto	if(time < OuterBasin.t_aqu, OuterBasin.sed_ned*OuterBasin.A_obj, 0.0)
	Upper regolith	M_tpi	if(time < OuterBasin.t_aqu, OuterBasin.water.M_bto, 0.0)
	Upper regolith	M_tpo	if(time < OuterBasin.t_aqu, OuterBasin.water.M_bti, 0.0)

			Outer	Inner	Central	
	Parameter		*t < t_aqu*	*t < t_aqu*	*t < t_aqu*	*t >= t_aqu*
Central	water	M_bti	3.0E+03	3.0E+03	3.0E+03	0
	water	M_bto	3.0E+03	3.0E+03	3.0E+03	0
	Upper regolith	M_tpi	3.0E+03	3.0E+03	3.0E+03	0
	Upper regolith	M_tpo	3.0E+03	3.0E+03	3.0E+03	0
Inner	Water	M_bti	3.0E+04	3.0E+04	0	0
	Water	M_bto	3.0E+04	3.0E+04	0	0
	Upper regolith	M_tpi	3.0E+04	3.0E+04	0	0
	Upper regolith	M_tpo	3.0E+04	3.0E+04	0	0
Outer	water	M_bti	3.0E+05	0	0	0
	water	M_bto	3.0E+05	0	0	0
	Upper regolith	M_tpi	3.0E+05	0	0	0
	Upper regolith	M_tpo	3.0E+05	0	0	0

Table 9. Solid material fluxes (kg year^{-1}) and their parameterisation (non-zero fluxes only). Mass transfers are set to dynamic equilibrium at the bed sediment of aquatic systems, sedimentation and resuspension rates are set equal. Accumulation of organic material during lake and wetland periods is assumed to be from atmospheric carbon via vegetation that is not included in the dynamic transport model.

Numerical data for basin and radionuclides

All nuclide specific data are taken from Nordén *et al*. (2010). Numerical values used in GEMA-Site are listed below.

NB. All data for concentration ratios (CR) are quoted in Nordén *et al*. in terms of (Bq kg carbon) (Bq kg^{-1} dry weight)$^{-1}$ for soil/sediment derived CRs or (Bq kg carbon) (Bq m^{-3})$^{-1}$ for water dwelling biota. Conversion of results for use in GEMA-site has been carried out before compilation of the GEMA-Site database in Ecolego, using the conversion factors discussed in Nordén *et al*.

Name	Unit	^{79}Se	^{94}Nb	^{129}I
Half life	Year	1130020	20300	1.57E+07
K_d inorganic material	$m^3\ kg^{-1}$	2.20E-02	1.90E+00	7.10E-03
K_d limnic ecosystem	$m^3\ kg^{-1}$	8.40E+00	2.30E+02	1.00E+01
K_d organic material	$m^3\ kg^{-1}$	5.30E-01	4.00E+01	7.10E-01
K_d sea ecosystems	$m^3\ kg^{-1}$	3.40E+00	2.00E+02	3.30E+00
CR cereal	kg dw kg^{-1} dw	2.27E+01	1.38E-02	1.16E-01
CR pasture	kg dw kg^{-1} dw	2.24E+01	2.04E-03	2.86E-01
CR root	kg dw kg^{-1} dw	1.99E+01	4.18E-03	1.02E-01
CR veg	kg dw kg^{-1} dw	3.42E+01	2.14E-02	3.11E-01
TR meat	d kg^1 fw	1.50E-02	2.60E-07	6.70E-03
TR milk	d kg^1 fw	4.00E-03	4.10E-07	5.40E-03
CR game	kg dw kg^{-1} dw	4.31E+01	4.57E-01	2.16E+00
CR mush	kg dw kg^{-1} dw	2.02E+01	1.84E-03	3.08E-02
CR natural	kg dw kg^{-1} dw	2.24E+01	2.04E-03	2.86E-01
CR crustacea	$m^3\ kg^{-1}$ dw	1.66E+01	2.81E+00	6.48E-01
CR fish freshwater	$m^3\ kg^{-1}$ dw	1.50E+01	9.68E-02	1.32E-01
CR fish sea	$m^3\ kg^{-1}$ dw	2.16E+01	7.65E-02	4.95E-02
Irrigation retention	unitless	5.00E-01	5.00E-01	5.00E-01
H_{ing}	Sv Bq^{-1}	2.90E-09	1.70E-09	1.10E-07
H_{inh}	Sv Bq^{-1}	6.80E-09	4.90E-08	9.80E-09
H_{ext}	(Sv $hour^{-1}$) (Bq m^{-3})$^{-1}$	3.00E-19	1.80E-13	1.80E-16

Name	Unit	Ra-226	Pb-210	Po-210
Half life	Year	1600	22.3	0.38
K_d inorganic material	$m^3\ kg^{-1}$	7.30E+00	7.70E+00	2.10E-01
K_d limnic ecosystem	$m^3\ kg^{-1}$	7.40E+00	5.40E+02	1.00E+01
K_d organic material	$m^3\ kg^{-1}$	2.30E+00	4.30E+01	6.60E+00
K_d sea ecosystems	$m^3\ kg^{-1}$	4.00E+00	2.50E+02	2.00E+04
CR cereal	kg dw kg^{-1} dw	1.69E-02	1.11E-02	2.36E-04
CR pasture	kg dw kg^{-1} dw	7.14E-02	1.07E-02	1.22E-01
CR root	kg dw kg^{-1} dw	1.02E-02	1.58E-03	2.81E-03
CR veg	kg dw kg^{-1} dw	1.38E-01	1.22E-01	1.12E-02
TR meat	d kg^{1} fw	1.70E-03	7.00E-04	5.00E-03
TR milk	d kg^{1} fw	3.80E-04	1.90E-04	2.10E-04
CR game	kg dw kg^{-1} dw	8.54E-01	8.11E-02	4.14E+01
CR mush	kg dw kg^{-1} dw	2.71E+00	1.20E-02	1.10E-01
CR natural	kg dw kg^{-1} dw	7.14E-02	1.07E-02	1.22E-01
CR crust	$m^3\ kg^{-1}$ dw	8.64E-02	1.66E+01	4.32E+01
CR fish fw	$m^3\ kg^{-1}$ dw	2.55E-02	1.19E-01	8.80E-01
CR fish sea	$m^3\ kg^{-1}$ dw	3.29E-01	2.12E-01	8.55E+00
Irrigation retention	unitless	2.00E+00	2.00E+00	2.00E+00
H_{ing}	Sv Bq^{-1}	2.80E-07	6.90E-07	1.20E-06
H_{inh}	Sv Bq^{-1}	9.50E-06	5.60E-06	4.30E-06
H_{ext}	(Sv $hour^{-1}$) (Bq m^{-3})$^{-1}$	5.60E-16	3.80E-17	9.50E-19

2015:47

The Swedish Radiation Safety Authority has a comprehensive responsibility to ensure that society is safe from the effects of radiation. The Authority works to achieve radiation safety in a number of areas: nuclear power, medical care as well as commercial products and services. The Authority also works to achieve protection from natural radiation and to increase the level of radiation safety internationally.

The Swedish Radiation Safety Authority works proactively and preventively to protect people and the environment from the harmful effects of radiation, now and in the future. The Authority issues regulations and supervises compliance, while also supporting research, providing training and information, and issuing advice. Often, activities involving radiation require licences issued by the Authority. The Swedish Radiation Safety Authority maintains emergency preparedness around the clock with the aim of limiting the aftermath of radiation accidents and the unintentional spreading of radioactive substances. The Authority participates in international co-operation in order to promote radiation safety and finances projects aiming to raise the level of radiation safety in certain Eastern European countries.

The Authority reports to the Ministry of the Environment and has around 300 employees with competencies in the fields of engineering, natural and behavioural sciences, law, economics and communications. We have received quality, environmental and working environment certification.

Strålsäkerhetsmyndigheten
Swedish Radiation Safety Authority

SE-171 16 Stockholm
Solna strandväg 96

Tel: +46 8 799 40 00
Fax: +46 8 799 40 10

E-mail: registrator@ssm.se
Web: stralsakerhetsmyndigheten.se